

UNLIMITED DISTRIBUTION

3



National Defence  
Research and  
Development Branch

Défense nationale  
Bureau de recherche  
et développement

AD-A178 296

TECHNICAL MEMORANDUM 87/202

January 1987

THIN-WALLED BEAM THEORIES  
AND THEIR APPLICATIONS IN  
THE TORSIONAL STRENGTH ANALYSIS  
OF SHIP HULLS

T.A. Vernon - Y. Nadeau

**DISTRIBUTION STATEMENT A**  
Approved for public release  
Distribution Unlimited

DTIC  
ELECTE  
MAR 26 1987  
S D

DTIC FILE COPY

Defence  
Research  
Establishment  
Atlantic



Centre de  
Recherches pour la  
Défense  
Atlantique

Canada

87 3 30 30

UNLIMITED DISTRIBUTION



**National Defence**  
Research and  
Development Branch

**Défense nationale**  
Bureau de recherche  
et développement

THIN-WALLED BEAM THEORIES  
AND THEIR APPLICATIONS IN  
THE TORSIONAL STRENGTH ANALYSIS  
OF SHIP HULLS

T.A. Vernon - Y. Nadeau

January 1987

Approved by B.F. Peters A/Director/Technology Division

DISTRIBUTION APPROVED BY

A/D/TO

TECHNICAL MEMORANDUM 87/202

Defence  
Research  
Establishment  
Atlantic



Centre de  
Recherches pour la  
Défense  
Atlantique

Canada

## Abstract

Unified developments of the St-Venant and warping-based thin-walled beam theories and their application in the torsional analysis of ship structures are presented. Open cell, closed cell and multi-cell configurations are treated. The warping-based torsional theory, which accounts for out-of-plane displacements and displacement restraints, provides axial stress distributions resulting from bimoments and in general offers improved predictions of shear stress distribution in thin-walled beams over the St-Venant theory; however, the use of that theory necessitates a more detailed cross-sectional property evaluation. The generalization of the warping function to a displacement field independent of the twist is discussed, as are several iterative methods of including warping shear deformations. The application of the prismatic warping theory to the analysis of non-prismatic beams is discussed, and the flexural-torsional beam method proposed by Pedersen is developed. This method, in conjunction with a computer program to calculate the required cross-sectional properties, has been integrated into a general torsional stress analysis capability within Defence Research Establishment Atlantic (DREA). The DREA system, which can account for geometric discontinuities in a structure, has been developed as an alternative to finite element methods, and is evaluated here via comparison with detailed finite element analyses for several prismatic beams with discontinuities. The flexural-torsional model appears to give representative behaviour only for structures which possess considerable transverse rigidity. Finally, the beam theory is applied to the stress analysis of the hull of a frigate. The shear and axial stresses predicted for the applied torsional load are quite low, despite the existence of significant geometric discontinuities in the hull.

Résumé

Sont présentés des développements unifiés de la théorie de Saint-Venant et de la théorie des poutres à paroi mince fondée sur le gauchissement ainsi que leur application à l'analyse torsionnelle des structures navales, pour des configurations à cellule ouverte, à cellule fermée et à cellules multiples. La théorie des torsions fondée sur le gauchissement, qui explique les déplacements hors-plan et les limites de déplacement, donne les distributions des contraintes axiales résultant des bimoments et, de façon générale, permet de mieux prévoir la distribution des contraintes de cisaillement dans les poutres à paroi mince que la théorie de Saint-Venant; elle nécessite toutefois une évaluation plus détaillée des caractéristiques sectionnelles. La généralisation de la fonction de gauchissement en un champ de déplacement indépendant de la torsion est étudiée, ainsi que plusieurs méthodes itératives d'inclusion des déformations de cisaillement de gauchissement. L'application de la théorie du gauchissement prismatique à l'analyse des poutres non prismatiques est également discutée, puis la méthode des poutres de fléchissement-torsion proposée par Pedersen est élaborée. Cette méthode, combinée à un programme de calcul des caractéristiques sectionnelles nécessaires, a été incorporée à un système d'analyse générale des contraintes torsionnelles au Centre de recherche pour la Défense/Atlantique (CRDA). Le système du CRDA, qui peut expliquer les discontinuités géométriques d'une structure, a été mis au point comme substitut aux méthodes à différences finies. Son évaluation est faite en comparaison avec des analyses détaillées à différences finies de plusieurs poutres prismatiques présentant des discontinuités. Le modèle fléchissement-torsion semble produire un comportement représentatif uniquement des structures qui possèdent une rigidité transversale considérable. Enfin, la théorie des poutres est appliquée à l'analyse des contraintes de la coque d'une frégate. Les contraintes axiales et de cisaillement prévues pour la charge torsionnelle appliquée sont assez faibles, en dépit de l'existence de discontinuités géométriques importantes dans la coque.



Accession For	
NTIS CRA&I	<input checked="" type="checkbox"/>
DTIC TAB	<input type="checkbox"/>
Unannounced	<input type="checkbox"/>
Justification	
By	
Distribution/	
Availability Codes	
Dist	Avail and/or Special
A-1	

# Contents

Abstract	ii
Table of Contents	iv
List of Figures	v
Notation	vi
<b>1 Introduction</b>	<b>1</b>
<b>2 A Review of the St-Venant Torsion Theory</b>	<b>3</b>
2.1 Open sections . . . . .	4
2.2 Closed section . . . . .	5
2.3 Multi-cell sections . . . . .	6
<b>3 Warping Torsion</b>	<b>8</b>
3.1 System of coordinates . . . . .	9
3.2 Open sections . . . . .	9
3.3 Closed sections . . . . .	17
3.4 Multi-cell sections . . . . .	20
3.5 A Refined Beam Torsion Model . . . . .	21
3.6 Account of Shear Deformation . . . . .	25
<b>4 Application to Non-Prismatic Beams</b>	<b>27</b>
4.1 General Approaches . . . . .	27
4.2 A Flexural-Torsional Model . . . . .	28
<b>5 Implementation and Evaluation of the Flexural-Torsional Model</b>	<b>34</b>
5.1 DREA Torsional Analysis Program Suite . . . . .	34
5.2 Evaluation of the torsional analysis system . . . . .	35
<b>6 Conclusion</b>	<b>37</b>
Appendix A - Notes on the Differential Equation	56
References	60
Bibliography	62

## List of Figures

1	Open, closed and multi-cell thin-walled beams. . . . .	40
2	Torsion restraints in a hull form with large discontinuities. . . . .	41
3	St-Venant shear stresses on open and closed sections. . . . .	41
4	Warping deformation of an open section. . . . .	42
5	Warping deformation of a closed section. . . . .	42
6	Equilibrium of internal and external forces on an unrestrained closed cell. . . . .	43
7	Shear flows in a multi-cell cross-section . . . . .	43
8	Global and local coordinate systems. . . . .	44
9	Generalized cross-sectional displacement definitions. . . . .	44
10	Forces on a wall segment. . . . .	45
11	Transfer of sectorial coordinate pole and origin. . . . .	45
12	Coordinate system for the flexural-torsional model. . . . .	46
13	Test 1: Simple box beam with discontinuity. . . . .	46
14	Twist angle predictions for test 1 under a torsional load (Pedersen). . . . .	47
15	Axial stress predictions for test 1 under a torsional load (Pedersen). . . . .	47
16	Test 2: Finite element model for comparison solution. . . . .	48
17	Twist angle predictions for test 2. . . . .	49
18	Axial stress predictions for test 2. . . . .	49
19	Axial stress contours of top surface showing stress concentration at the discontinuity. . . . .	50
20	Moment distribution applied to the frigate hull. . . . .	50
21	Twist angle prediction for the frigate hull. . . . .	51
22	Axial stress immediately aft of the major discontinuity in the frigate hull . . . . .	52
23	Axial stress immediately forward of the major discontinuity in the frigate hull. . . . .	53
24	Shear stress distribution from a traditional analysis for a cross-section of the frigate hull. . . . .	54
25	Shear stress distribution from the warping based methods for a cross-section of the frigate hull. . . . .	55
A1	Axial stress distribution for various $k$ values in a clamped-free beam under a concentrated end moment. . . . .	59

## Notation

$A$	cross-section area
$b$	length of discrete thin wall segment
$B$	hull breadth
$c_y, c_z$	coordinates of cross-section pole (shear center)
$C_W$	hull waterplane area coefficient
$C_B$	hull block coefficient
$D$	hull depth, vector of generalized displacements
$E$	modulus of elasticity
$G$	shear modulus
$h$	distance from profile line tangent to shear center
$I_y$	second moment of area about the Y-axis
$I_z$	second moment of area about the Z-axis
$I_{yz}$	product of area
$I_{\omega\omega}$	$\int \omega^2 dA$ sectorial moment of area
$I_{y\omega}$	$\int \omega y dA$ sectorial deviation moment
$I_{z\omega}$	$\int \omega z dA$ sectorial deviation moment
$I_{hh}$	$\int h^2 dA$ central moment of area
$I_t$	St-Venant torsional constant
$k$	warping parameter $= l \sqrt{\frac{GI_t}{EI_{\omega\omega}}}$
$l$	length of beam
$L$	total hull length
$m, m_x, m_z$	distributed torsional and flexural moments
$M_\omega$	bimoment

$n$	number of segments in the cross-section
$nc$	number of cells in a cross-section
$p_x, p_y, p_z$	distributed body forces
$P_x, P_y, P_z$	concentrated body forces
$P(x)$	particular solution of a differential equation
$q_1, q_2$	St-Venant shear flow, warping torsional shear flow
$Q_y, Q_z$	shear forces along y and z axes respectively
$\bar{q}$	normalized St-Venant shear flow
$s$	curvilinear coordinate along wall profile
$s_0, s_1$	arbitrary and principal curvilinear coordinate origins
$S_y$	static moment = $\int y dA$
$S_z$	static moment = $\int z dA$
$S_w$	static moment = $\int w dA$
$\bar{S}_y$	static moment function = $\int_0^s yt ds$
$\bar{S}_z$	static moment function = $\int_0^s zt ds$
$\bar{S}_w$	static moment function = $\int_0^s \omega t ds$
$t$	wall thickness
$T$	total torsional moment about shear center, kinetic energy
$T_s$	St-Venant torsional moment
$T_w$	warping torsional moment
$u$	normal displacement with respect to the profile line
$U$	internal energy
$v$	tangential displacement along the profile line
$w$	longitudinal displacement

$W$	potential energy of the loads
$x$	longitudinal coordinate
$X_e$	vector of integrable functions
$y, z$	cartesian coordinates in the plane of the cross-section
$\alpha_1^i, \alpha_2^i$	warping compatibility coefficients at station $i$
$\beta$	horizontal bending slope
$\gamma$	shear strain in cross-section wall
$\delta$	longitudinal deformation due to axial loads at a section
$\epsilon$	engineering strain, shear center offset
$\eta$	vertical offset of a point from longitudinal axis
$\theta$	warping factor
$\kappa$	general coefficient matrix
$\xi$	horizontal offset of a point from longitudinal axis
$\rho$	warping moment parameter = $\frac{I_{hh}}{I_{hh} - I_t}$
$\sigma_x$	warping normal stress
$\tau$	general shear stress
$\bar{\tau}$	normalized St-Venant shear stress
$\tau_1$	St-Venant shear stress
$\tau_2$	warping shear stress
$\phi$	rotational angle
$\phi'$	rotation per unit length (twist)
$\omega$	sectorial coordinate
$\Omega$	frequency
$\Psi$	phase angle
$\dot{\omega}(s)$	sectorial derivative = $\frac{\partial \omega}{\partial s}$

## 1 Introduction

Thin-walled beams have found many applications in modern structural engineering because of their potentially high strength/weight ratios. Much of the early development of engineering thin-walled beam theory has its roots in aircraft design and analysis, where weight savings have always been particularly important. Similar methods have traditionally been applied in the stress and vibration analysis of ship hulls, as these structures, although of a different scale, are well within the dimensional assumptions of the thin-walled theory.

The construction of larger and more novel hull forms in the past two decades has led to a demand for better analytical tools for the prediction of ship hull flexural and torsional response. While numerical techniques such as the finite element method can provide the desired capability, the time consuming nature of that form of analysis has provided motivation for further development of thin-walled beam modelling methods. These more recent developments in the thin-walled beam theory are the subject of this report.

There are two inherent characteristics of thin-walled beams which can be a drawback to their utilization: the higher level of shear stress which is generally present in the thin walls, and the tendency of such beams to warp out of plane under torsional or flexural loading. The higher wall stresses can lead to shear buckling of very thin plate structures, a particular concern in the aerospace industry, but not generally a problem with ships because of their greater plate thicknesses. The warping tendency is particularly severe in the case of torsional loading of open cell sections, Figure 1, a cross-sectional configuration common in ship hulls. In such cases, the application of the traditional St-Venant theory of torsion can lead to inaccurate stress predictions. This inadequacy is primarily a result of the neglect of the warping deformation, which is a function of the geometry of the section in much the same manner as bending is related to the area moments of the section. In attempting to obtain a better stress prediction capability, the modern beam models for torsional analysis account for warping.

As suggested, the requirement for a detailed torsional analysis capability for ship hulls is relatively recent. Most conventional hulls have adequate torsional resistance simply as a result of the closed, cellular configuration of the shell and decks, or from the inclusion of torsion boxes, Figure 2. However, if the cellular nature of the hull is highly discontinuous, or if large sections of the hull are open, torsional loading can induce quite high shear and localized axial stresses in the vicinity of the geometric discontinuities, and deformations can be high in the open sections. This has been a significant consideration in the design of second and third generation container ships, and torsional analysis methods for ship structures have been developed to assess displacements and stresses in such designs. These methods also have applications in the design and analysis of modern warship hulls which often have large discontinuities and open sections to accommodate uptakes and downtakes,

weapon systems, or elevator shafts. Prismatic beam torsion theories are generally used, whereby the hull is modelled as a series of prismatic segments. With a consistent derivation of the coupling and compatibility parameters required for linking the beam segments, these simpler models can provide stress predictions which compare reasonably well with full scale finite element and experimental results. However, in certain cases, the assumptions on which these theories are generally based are not valid, and the beam theory predictions are little better than poor approximations of the true structural response. Unfortunately, the relaxation of the violated assumptions often leads to an intractable solution method for the complex geometries of ship cross-sections.

The available comprehensive literature on this subject originates mainly from German and northern European authors, but much of this is lacking in general context and tends to be problem specific. As well, the notation is inconsistent and the mathematical development, with few exceptions, is often vague and incomplete. With these considerations, the aim of this report is to provide a unified development of both the St-Venant and warping torsion theory, emphasizing the different assumptions underlying each model. The development treats open, closed and multi-cell configurations separately for both theories and also presents the further refinement of the warping torsional model proposed by Kollbrunner and Hajdin<sup>(1)</sup> and discusses the iterative techniques suggested by Westin<sup>(2)</sup> and Pittaluga<sup>(3)</sup>. Section 2 presents a review of the St-Venant theory, and the warping theory is developed in Section 3.

Although warping based theories can provide quite adequate displacement and stress predictions for prismatic beams, many structures of interest, such as ship hulls, are non-prismatic. Methods of treating this problem are discussed in Section 4. As an example of the warping theory generalized to include longitudinal cross-sectional property variation, the formulation of the differential equations of equilibrium as proposed by Pedersen<sup>(4)</sup> is also presented in Section 4. This method, which models horizontal beam flexure and torsional displacements, also accounts for larger geometric discontinuities in the structure via coupling coefficients relating the bending and warping functions on either side of a discontinuity. The large cutouts for intakes and uptakes in warship hulls are examples of such discontinuities.

A modified version of the flexural-torsional solution algorithm presented in Section 4 is used in conjunction with several programs developed at Defence Research Establishment Atlantic (DREA) to provide a simpler alternative to finite element analyses of thin-walled structures under torsional loading. This system, described in Section 5, utilizes the TPGEOM<sup>(5)</sup> program to establish a cross-sectional data base for a structure, and the SCRAP<sup>(6)</sup> program for calculation of all relevant cross-sectional properties. These properties are stored by section, and a beam model is constructed for use in the formation of the equilibrium equations. The sectional shear and axial stress distributions are also calculated and displayed by the SCRAP program. These distributions are scaled from the internal forces in the beam calculated from the TORSON program, which provides a nu-

merical solution of the coupled differential equilibrium equations. The TORSON program was originally obtained from the Technical University of Denmark.

Section 5 also describes an evaluation of the displacement and stress prediction capabilities of this system by comparative analyses utilizing detailed finite element models for several simple prismatic thin-walled beams. These studies have indicated that the assumption inherent in the beam methods of no in-plane distortion is a very critical one, a conclusion also reached by other authors.<sup>(2,7)</sup> Although potentially very significant in unstiffened structures, the loss of accuracy due to cross-sectional distortion will be reasonably nominal in a beam method analysis of a typical warship hull because of the large configurational stability provided by the numerous deep web frames and transverse bulkheads. The system has been utilized in a study of a frigate under an assumed torsional/flexural load, the results of which are also presented in Section 5. Since no comparative solution exists for this hull, these results remain unverified.

## 2 A Review of the St-Venant Torsion Theory

Traditional torsional analyses of ship hulls have utilized the St-Venant theory of torsion to predict the shear stresses and twist angles of the hull girder under a specified loading distribution.<sup>(8)</sup> If the hull sections are largely cellular in nature, the shear stress and twist angles will generally be small, and their predictions via the traditional methods can be considered accurate to at least the same level as the description of the loads. If the structure is of a mainly open or mixed nature, the stress predictions from the St-Venant theory can be in error, particularly in the vicinity of large geometric discontinuities or longitudinal displacement restraints such as torsion boxes, which cannot be properly included in that approach. These discontinuities and stiffening structures inhibit the free warping of the structure, and can lead to significant axial and secondary shear stresses superimposed on the St-Venant shear stress distribution. An example of the influence of a discontinuity on the stress distribution near the discontinuity of a typical ship hull is presented in the final section of this report.

A physical concept of the phenomenon of warping is useful in visualizing the difference between classical torsion (St-Venant) and warping torsion. Subsequent discussion will present the mathematical treatment of these two subjects.

A St-Venant torsional moment generates a shear stress pattern on the surface of the cross-section as illustrated in Figure 3. For a closed section, a shear flow is able to 'circulate' around the cross-section and the shear stress is constant over the thickness. For an open section, the shear stress assumes a linear distribution over the thickness with a zero average. The notion of St-Venant torsional stiffness can thus be considered as the effectiveness with which a given cross-section will generate a shear stress distribution on its surface to oppose

the applied torsional moment.

To illustrate warping torsion, consider an open beam section, Figure 4. The cross-section undergoing rigid body rotation must also undergo longitudinal displacement as a kinematical consequence of this rotation. In other words, the tangential displacement of an element of the surface of the cross-section must be accompanied by a longitudinal displacement  $w$  if the generator  $G$  is not to stretch. If this longitudinal displacement is restrained, a new resistance will have to be countered to deform the body, adding to the overall torsional stiffness. Additional stresses will thus be induced in the beam. Accordingly, the warping torsional stiffness of a cross-section can be viewed as the relative capacity of the section to generate a stress pattern on its surface that will effectively resist a torsional moment when the section is longitudinally restrained.

As discussed, a shear flow is free to circulate around the contour of a closed section. Observing an element of the wall, Figure 5, it can be seen that equilibrium then requires a longitudinal shear flow. This will cause a shear deformation in the plane of the wall and this deformation will partially cancel the warping. For this reason, the warping displacement in closed sections will be smaller and consequently less affected by a longitudinal restraint. Hence, closed sections will generally have a smaller warping torsional stiffness than open sections. For certain geometries such as squares and circles, the shear and kinematic deformation completely cancel each other, and no warping occurs.

The St-Venant theory of torsion assumes that the section is free to warp. For elastic behaviour, a first order differential equation can be derived,<sup>(9)</sup> which relates the St-Venant torsional moment to the twist,

$$T_s = G I_t \phi' \quad (1)$$

where  $T_s$  is the St-Venant torsional moment,  $G$  is the shear modulus of the material,  $I_t$  is the St-Venant torsional constant of the section, and  $\phi'$  is the twist (rotation per unit length). This relationship is valid for both open and closed cell configurations; the only difference occurs in the value of  $I_t$ , the St-Venant torsional constant. The calculation of this constant for the cases of open, closed and multicell sections is briefly presented below.

## 2.1 Open sections

For an open section generated from a series of folded segments,  $I_t$  can be approximated<sup>(10)</sup> as  $I_t^o$ , where,

$$I_t^o = \frac{1}{3} \int_0^b t^3 ds \quad (2)$$

or, for numerical calculation,

$$I_t^o = \frac{1}{3} \sum_{i=1}^n b_i t_i^3 \quad (3)$$

where  $b$  and  $t$  are respectively the length and the thickness of the  $n$  discretized elements of the cross-section. The stress has a linear variation over the thickness with a zero mean, and its maximum value at the edge is approximated by,

$$(\tau_1^o)_{max} = \frac{T_s t}{I_t^o} \quad (4)$$

## 2.2 Closed section

A closed section is considered here to be a single cell cross-section of arbitrary shape that contains no free ends. For such a section, the torsional constant is composed of two terms:

- (1)  $I_t^o$ , as for an open section and corresponding again to a shear stress varying linearly over the thickness;
- (2)  $I_t^c$ , corresponding to a shear stress which is constant over the thickness.

The closed cell torsional constant  $I_t^c$  can be found from consideration of the overall equilibrium and potential energy. Consider an element of the wall that can be of varying thickness, Figure 6. Since the section is assumed to be free of longitudinal restraint, there should be no axial stress on the surface. Equilibrium in the axial direction requires,

$$(\tau_b t_b - \tau_a t_a) dx = 0 \quad (5)$$

which implies, for  $\tau t = q$ , that

$$q_a = q_b \quad (6)$$

indicating that the shear flow must be constant around the section. It should be noted that this conclusion was reached because of the assumption of no axial stress over the thickness. This is an important characteristic of St-Venant torsion that differs from warping torsion, as will be shown.

Referring to Figure 6, the value of the St-Venant shear flow  $q_1$  can be found from the equilibrium of internal and external forces. We have,

$$dT_s = h q_1 ds \quad (7)$$

since

$$dA = \frac{1}{2} h ds \quad (8)$$

We have, after integration,

$$T_s = 2 q_1 A \quad (9)$$

and hence,

$$q_1 = \frac{T_s}{2A} \quad (10)$$

The work done by the applied forces must equal the work done by the internal forces.

$$\frac{1}{2}T_s d\phi = dx \oint r_1 \gamma t ds \quad (11)$$

since

$$\gamma = \frac{\tau_1}{G} \quad (12)$$

$$T_s d\phi = dx \oint \frac{(r_1)^2}{G} t ds \quad (13)$$

where the  $\oint$  indicates integration around the complete cell. Substituting equation (13) into equation (10) gives,

$$T_s = G I_t^c \phi' \quad (14)$$

where,

$$I_t^c = \frac{4A^2}{\oint \frac{ds}{t}} \quad (15)$$

In most sections containing closed cells,  $I_t^c$  is many orders of magnitude larger than  $I_t^o$ , and the latter is generally neglected.

### 2.3 Multi-cell sections

For a section composed of a number of cells, the total St-Venant torque will be equal to the sum of the torques contributed by each cell,

$$T_s = \sum_{i=1}^{nc} 2(Aq_1)_i \quad (16)$$

This indeterminate problem can be solved by assuming that the shape of the section is assumed to remain unchanged. This implies that all cells have the same twist,

$$\phi'_1 = \phi'_2 = \phi'_3 \dots = \phi'_{nc} = \phi' \quad (17)$$

From equation (13), the twist can be expressed as,

$$\phi'_i = \frac{1}{2A_i G} \oint_i \frac{(q_1)_i}{t} ds \quad (18)$$

Letting

$$\bar{q}_i = \frac{(q_1)_i}{\phi'} \quad (19)$$

we obtain the system of equations,

$$\oint_i \frac{\bar{q}_i}{t} ds = 2A_i G \quad i = 1, nc \quad (20)$$

Developing the integral for cell  $i$  gives,

$$\bar{q}_i \oint_i \frac{ds}{t} - \bar{q}_j \int_{ij} \frac{ds}{t} - \bar{q}_k \int_{ik} \frac{ds}{t} \dots = 2A_i G \quad (21)$$

where  $\bar{q}_i$  and  $\bar{q}_j$  are the constant unit shear flows around cell  $i$  and  $j$ , respectively and  $\int_{ij}$  represents an integration performed along walls common to cell  $i$  and  $j$ , Figure 7. The integrals in the above expression can readily be calculated by a cross-sectional analysis program, and equation (20) can be expressed as a matrix system for numerical computation as,

$$[\kappa] (\bar{q}) = 2G (A) \quad (22)$$

where,

$$\kappa_{ii} = \sum_{\text{cell } i} \frac{ds}{t} \quad (23)$$

$$\kappa_{ij} = \sum_{ij} \frac{ds}{t} \quad (24)$$

Equation (16) then becomes,

$$T_s = \sum_{i=1}^{nc} 2A_i (2\phi' G [\kappa]^{-1} (A))_i \quad (25)$$

Rearranging,

$$T_s = G I_t \phi' \quad (26)$$

where,

$$I_t = 4(A) [\kappa]^{-1} (A) \quad (27)$$

For a specified  $T_s$ , the twist can be obtained and the St-Venant shear flows  $(q_1)_i$  found from,

$$(q_1)_i = \bar{q}_i \phi' \quad i = 1, nc \quad (28)$$

in which  $\bar{q}_i$  has been obtained from the solution of the matrix system of equation (22). It can be observed that equation (27) is simply the general form of equation (15).

Although not discussed here, the calculation of the shear stress distribution for multi-cell sections under transverse shear loads follows a similar procedure to that outlined above. In that case, a zero twist is assumed for each cell and the shear flow is written as the sum of an 'open' cell shear flow and a constant correcting flow. An analogous matrix system relating the open and correcting shear flows can be developed, which utilizes the same coefficient matrix  $[\kappa]$  as above (see, for example, Reference 11).

### 3 Warping Torsion

The St-Venant theory of torsion discussed in the previous section has been widely used to predict shear stresses in beams, and the assumptions on which it is based are realistically accurate for thick-walled or solid sections, or sections which have no warping restraint. In the case of thin-walled sections, the assumption of free warping is often a poor one for two reasons. The first is that such sections are prone to warp and the second is that this warping is usually restrained in some way. These restraints provide additional torsional stiffness but generate secondary shear stresses in the vicinity of the restraint which can alter the overall stress distribution significantly.

Warping restraints are typically points of global fixity or internal points of attachment of restraining structure. In non-prismatic beams, the geometric discontinuities themselves are relative restraints, and the incompatibility occurring in the warping displacements can lead to additional shear and axial stresses. In the case of ship hulls, such discontinuities exist at large hatch openings, and wherever cellular sections abut open sections. As with other forms of loading, abrupt changes in geometry generate stress concentrations.

Whereas the St-Venant theory provided a simple first order differential equation relating the applied load and displacement, it will be shown that the inclusion of warping results in a fourth order differential equation. This equation must be solved for the distribution of twist and its derivatives to obtain sectional stresses in the beam. This section presents the derivation of the equation for a prismatic beam. Two assumptions underlie all of the developments that follow:

- (1) The beams contain only thin walls. Accordingly, warping displacements and stresses can be assumed constant over the wall thickness.
- (2) The shape of the cross-section remains unchanged; no transverse deformation occurs in the cross-sectional plane under the applied load.

A third assumption will often be made about the shear deformation in the plane of the walls. It will be outlined as each case arises.

The development is in two parts; the first treats open sections and draws heavily on the

development of Vlasov,<sup>(12)</sup> and the second treats closed configurations. For the simplest case of an open section, warping torsion will be studied in parallel with other states of loading since bending and warping torsion are similar in their mathematical formulation. Thus, the latter can be understood as part of a general theory of thin-walled beams. As more complicated cases are treated, the development will consider warping torsion only. Finally, multi-cell sections are presented as a generalization of the closed cell development.

### 3.1 System of coordinates

A right-handed system of coordinates will be used, Figure 8, with the cross-section in the  $Y - Z$  plane,  $Z$  vertical, and axis  $O - X$  being any axis of the beam parallel to the axis of the centroid. Each point on the surface of the cross-section can therefore be determined by the two coordinates  $y$  and  $z$ . Because the beam is thin-walled, a more convenient coordinate,  $s$ , can be defined as the curvilinear distance along the wall profile from an arbitrary origin. In this case, the positive direction is taken as counterclockwise with respect to the origin of the cartesian system of coordinates. Once the origin of the  $s$ -coordinate is established, the functions  $y(s)$  and  $z(s)$  are well-defined for the complete cross-section.

### 3.2 Open sections

For open sections, an assumption ( $3^a$ ) in addition to (1) and (2) above is made:

( $3^a$ ) The shear deformation  $\gamma$ , in the plane of the walls (plane  $zs$  of Figure 6) can be neglected.

It was stated in the previous chapter that for an open section, there is no St-Venant shear flow circulating around the cross-section. Instead, the shear stress assumes a linear distribution over the thickness with a zero average. Consequently, equilibrium of a wall element does not require longitudinal shear stress and there will be no longitudinal shear deformation caused by a St-Venant torsional moment. In the case of warping torsion, the warping shear stress will be assumed constant over the thickness, in accordance with assumption (1). As a result, there will be a certain amount of shear deformation in the plane of the walls caused by a warping torsional moment. Therefore, the consequence of assumption ( $3^a$ ) is the neglect of the longitudinal shear deformation but not the longitudinal shear stress nor the axial deformation caused by a warping torsional moment.

With reference to Figure 9, the displacement of any point on the cross-section can be expressed with respect to the displacement of an arbitrarily chosen point  $A$ , which is assumed to be rigidly connected to the cross-section. In the figure,  $\xi(x)$  and  $\eta(x)$  represent the projections of the rigid body displacement of point  $A$  on axis  $O - Y$  and  $O - Z$  respectively

for a given section, for  $x$  constant. These functions of  $x$  then represent the space curve that an axis of the beam passing through point  $A$  assumes after deformation.

Let  $\phi(x)$  be the rotation of the section in its own plane ( $Y - Z$ ). The displacement in the plane of the cross section of any point  $B$  located on its surface can be expressed using assumption (2), which allows us to treat the cross-section as a rigid body. The kinematics of rigid body motion can therefore be applied, giving,

$$\xi_b = \xi(x) - (z_b - a_z)\phi(x) \quad (29)$$

$$\eta_b = \eta(x) - (y_b - a_y)\phi(x) \quad (30)$$

The general vector representing the displacement of point  $B$  can be expressed using the three components  $u$ ,  $v$ ,  $w$ , as illustrated in Figure 8. Displacement  $u$  is directed along the tangent to the profile line with positive direction given by the  $s$  coordinate;  $w$  is directed along the axis of the beam with positive direction given by the  $X$ -axis;  $v$  is directed along the normal to the profile line with positive direction given by the requirement that vectors  $u$ ,  $v$ ,  $w$  form a right-handed coordinate system.

Let  $\alpha(s)$  be the angle that the tangent to the profile line makes with the  $0 - Y$  axis, Figure 9. Let  $h(s)$  and  $g(s)$  be the length of the perpendiculars from point  $A$  to the tangent and normal of the profile line respectively, at point  $B$ . Components  $u$  and  $v$  can be found from equation (29) and geometrical considerations, giving,

$$u(x, s) = -\xi(x) \cos \alpha(s) - \eta(x) \sin \alpha(s) + \phi(x)h(s) \quad (31)$$

$$v(x, s) = -\xi(x) \sin \alpha(s) + \eta(x) \cos \alpha(s) + \phi(x)g(s) \quad (32)$$

To this point, only kinematic relations have been used, giving the state of displacement in the  $Y - Z$  plane. It remains to determine the longitudinal displacement  $w$ . To do so, use will be made of assumption (3<sup>a</sup>) of negligible shear strain in the walls of the beam. Expressed mathematically, this condition is,

$$\frac{\partial u}{\partial x} + \frac{\partial w}{\partial s} = \gamma_{xs} = 0 \quad (33)$$

Solving equation (33) for  $w$  yields,

$$w(x, s) = \delta(x) - \int_{s_0}^s \frac{\partial u}{\partial x} ds \quad (34)$$

where  $\delta(x)$  is the longitudinal displacement of the cross-section at point  $s_0$  of the  $s$ -coordinate.

Equation (31) gives,

$$\frac{\partial u}{\partial x} ds = -\xi'(x) \cos \alpha(s) ds - \eta'(x) \sin \alpha(s) ds + \phi'(x)h(s) ds \quad (35)$$

where the prime notation indicates differentiation with respect to  $x$ . Observing that,

$$\cos \alpha(s) ds = -dy \quad (36)$$

$$\sin \alpha(s) ds = -dz \quad (37)$$

and defining,

$$h(s) ds = d\omega \quad (38)$$

substitution of equations (35), (36) and (38) into (34) yields, after integration,

$$w(x, s) = \delta(x) - \xi'(x)y(s) - \eta'(x)z(s) - \phi'\omega(s) \quad (39)$$

For specific points  $A$  and  $s_0$ ,  $\omega(s)$  is a uniquely defined function of  $s$ , just as  $y(s)$  and  $z(s)$  and, in fact,  $\omega(s)$  corresponds to twice the area of the triangle formed by points  $A$ ,  $s_0$  and  $s$ . This function of  $s$  is commonly called the sectorial coordinate, point  $A$  is called the pole of the sectorial coordinate and point  $s_0$  is the sectorial origin. The line that connects point  $A$  to point  $s_0$  is defined as the fixed radius vector and the line that connects point  $A$  to the variable  $s$  is defined as the mobile radius vector. These vectors define the sign convention used for the integrations involved in the calculation of cross-sectional properties. A contour increment is considered here to be positive if the mobile radius vector moves counterclockwise. This sign convention can be included in the definition of the sectorial coordinate, equation (38), if the  $s$ -coordinate is chosen in the proper fashion; that is, if its positive direction defines a counterclockwise movement with respect to pole  $A$ .

The first term of equation (39) represents a uniform axial stretching, and the second and third terms represent bending of the beam. The last term is due to the warping of the cross-section under torsion, and represents the displacement of the cross-section out-of-plane. The similarity of the bending and warping terms is evident and this analogy is useful in dealing with the less familiar problem of warping torsion.

For elastic behaviour, the axial stress in the beam is given by:

$$\sigma_x = E\epsilon_x = E \frac{\partial w}{\partial x} \quad (40)$$

Substituting from equation (39),

$$\sigma_x(x, s) = E(\delta'(x) - \xi''(x)y(s) - \eta''(x)z(s) - \phi''(x)\omega(s)) \quad (41)$$

The tangential shear flow is found using the condition of equilibrium of a wall element, Figure 10. If there are no body forces,

$$t \frac{\partial \sigma_x}{\partial x} + t \frac{\partial \tau_{xs}}{\partial s} = 0 \quad (42)$$

Then,

$$t\tau_{zs} = - \int_0^s \frac{\partial \sigma_z}{\partial x} t \, ds + (tr)_0 \quad (43)$$

If the integration is commenced at a free edge,  $(tr)_0$  is zero. Substituting equation (41) into (43) and integrating gives the shear flow as,

$$t\tau_{zs} = q(x, s) = E(-\delta''(x)\bar{F}(s) + \xi'''(x)\bar{S}_y(s) + \eta'''(x)\bar{S}_z(s) + \phi'''(x)\bar{S}_\omega(s)) \quad (44)$$

where,

$$\bar{F}(s) = \int_0^s t \, ds \quad (45)$$

$$\bar{S}_y(s) = \int_0^s yt \, ds \quad (46)$$

$$\bar{S}_z(s) = \int_0^s zt \, ds \quad (47)$$

$$\bar{S}_\omega(s) = \int_0^s \omega t \, ds \quad (48)$$

These quantities, called static moments functions, are determined from an integration commenced at a free edge, following an integration path that leads inward in the section. The condition of a zero algebraic sum of the shear flows is used at segment intersections (nodes) to continue the integration. For the case of pure torsion, the shear stress of equation (44) is often referred to as the secondary shear stress  $\tau_2$ , where,

$$t\tau_2 = q_2 = E\phi'''(x)\bar{S}_\omega(x) \quad (49)$$

The derivation of this stress assumes that an axial stress exists in the wall. In the previous chapter, the St-Venant shear stress was found assuming the absence of any normal stress; therefore, these two stresses are of a different nature. The St-Venant shear stress is commonly called the primary shear stress  $\tau_1$ . The total shear stress is the sum of  $\tau_1$  and  $\tau_2$ , and the relative distributions are functions of the geometric properties and the warping restraints in the system. In an open section, the total shear stress is then the superposition of a constant and linearly varying distribution across the wall thickness.

In the development of  $\sigma(x)$  and  $\tau_{zs}$ , four unknowns are included:  $\delta(x)$ ,  $\xi(x)$ ,  $\eta(x)$  and  $\phi(x)$ . These unknowns can be found from the requirement of equilibrium of the complete beam.

Consider a strip of the beam of length  $dx$ , Figure 10. From equilibrium, we have,

$$\sum F_x = 0 \quad \int_A \frac{\partial(\sigma_z t)}{\partial x} dx \, ds + p_x dx = 0 \quad (50)$$

$$\sum F_y = 0 \quad \int_A \frac{\partial(\tau t)}{\partial x} \cos \alpha \, dx \, ds + p_y \, dx = 0 \quad (51)$$

$$\sum F_z = 0 \quad \int_A \frac{\partial(\tau t)}{\partial x} \sin \alpha \, dx \, ds + p_z \, dx = 0 \quad (52)$$

$$\sum M_A = 0 \quad \int_A \frac{\partial(\tau t)}{\partial x} h \, dx \, ds + m \, dx + T_s = 0 \quad (53)$$

Here,  $p_x$ ,  $p_y$  and  $p_z$  are the distributed forces acting on the section, and  $m$  is the total distributed torsional moment. Since the St-Venant shear stress is not included in  $\tau$ , its resulting moment, the St-Venant torsional moment  $T_s$ , can be introduced separately in the equilibrium equations. Dividing equations (50)-(53) by  $dx$  and using equation (36), we can integrate by parts to obtain,

$$\int_A \frac{\partial \sigma_x}{\partial x} \, dA + p_x = 0 \quad (54)$$

$$\left[ \frac{\partial(\tau t)}{\partial x} y \right]_A - \int_A y \frac{\partial}{\partial s} \left[ \frac{\partial(\tau t)}{\partial x} \right] + p_y = 0 \quad (55)$$

$$\left[ \frac{\partial(\tau t)}{\partial x} z \right]_A - \int_A z \frac{\partial}{\partial s} \left[ \frac{\partial(\tau t)}{\partial x} \right] + p_z = 0 \quad (56)$$

$$\left[ \frac{\partial(\tau t)}{\partial x} \omega \right]_A - \int_A \omega \frac{\partial}{\partial s} \left[ \frac{\partial(\tau t)}{\partial x} \right] + m + \frac{dT_s}{dx} = 0 \quad (57)$$

where  $dA = t \, ds$ .

The first component of the last three equations is evaluated on the limits of the surface, the free edges. These terms all vanish identically since  $\frac{\partial \tau(x)}{\partial x} = 0$  on a free edge where  $\tau(x)$  is zero everywhere. Substituting from equations (41) and (44) for  $\sigma$  and  $\tau$ , we have, after rearrangement,

$$-A\delta'' + S_y \xi'''' + S_z \eta'''' + S_\omega \phi'' = \frac{p_x}{E} \quad (58)$$

$$S_y \delta'''' + I_x \xi'''' + I_{yz} \eta'''' + I_{\omega y} \phi'''' = \frac{p_y}{E} \quad (59)$$

$$S_z \delta'''' + I_{yz} \xi'''' + I_y \eta'''' + I_{\omega z} \phi'''' = \frac{p_z}{E} \quad (60)$$

$$S_\omega \delta'''' + I_{\omega y} \xi'''' + I_{\omega z} \eta'''' + I_{\omega \omega} \phi'''' = \frac{m}{E} + \frac{GI_t}{E} \phi'' \quad (61)$$

Equations (58)-(61) are derived for an arbitrary coordinate system but can be more conveniently expressed if a coordinate system is chosen such that,

$$S_y = S_z = I_{yz} = 0 \quad (62)$$

and,

$$S_\omega = I_{\omega y} = I_{\omega z} = 0 \quad (63)$$

Equation (62) is satisfied if coordinates  $y$  and  $z$  are expressed in terms of the principal axes of the section. The requirements of equation (63) define the pole and the origin of the principal sectorial coordinate. Assume point C, Figure 11, is a pole that fulfills these conditions. The sectorial coordinate with respect to pole C can be expressed as a function of the sectorial coordinate with respect to an arbitrary pole A by geometric relations,

$$\omega_C = \omega_A + (c_x - a_x)y(s) - (c_y - a_y)z(s) + (c_y - a_y)z(s_0) - (c_x - a_x)y(s_0) \quad (64)$$

where  $y(s_0)$  and  $z(s_0)$  are the coordinates of the sectorial origin for both poles ( $\omega_C(s_0) = \omega_A(s_0) = 0$ ). Multiplying by the functions  $y(s)$  and  $z(s)$  in turn, and integrating both equations over the sectional area, these relations reduce to,

$$(c_x - a_x)I_x + \int_A \omega_A y \, dA = 0 \quad (65)$$

$$-(c_y - a_y)I_y + \int_A \omega_A z \, dA = 0 \quad (66)$$

The coordinates of the principal pole at C are then,

$$c_y = a_y + \frac{I_{\omega_A z}}{I_y} \quad (67)$$

$$c_x = a_x + \frac{I_{\omega_A y}}{I_x} \quad (68)$$

It can be shown that the principal pole of the sectorial coordinate is also the shear center of the section<sup>(12)</sup>.

The principal sectorial origin  $s_1$  can be found from the requirement that  $S_\omega = 0$  in that system. Using the geometry of Figure 11, we can express the sectorial coordinate with origin at  $s_1$  as a function of the coordinate with origin at an arbitrary point  $s_0$  as,

$$\omega(s_1, s) = \omega(s_0, s) - \omega(s_0, s_1) \quad (69)$$

where it is now assumed that  $\omega$  is calculated with respect to the principal pole. Multiplying the above expression by  $dA$ , applying the above vanishing criterion, and integrating over the sectional area gives  $\omega(s_0, s_1)$  as,

$$\omega(s_0, s_1) = \frac{1}{A} S_\omega(s_0, s) \quad (70)$$

We can use equations (69) and (70) to redefine the sectional properties in terms of this principal sectorial coordinate. Using this system, the set of equations (58)-(61) reduces to the more familiar form,

$$EA\delta'' = -p_x \quad (71)$$

$$EI_z\xi'''' = p_y \quad (72)$$

$$EI_z\eta'''' = p_z \quad (73)$$

$$EI_{\omega\omega}\phi'''' - GI_t\phi'' = m \quad (74)$$

It is instructive to define generalized forces in terms of the global degrees of freedom of the beam: longitudinal stretching, bending in the two directions and twist. Accordingly, these forces can be defined as the work done by the stress fields of  $\sigma$  and  $\tau$  moving through a unit global displacement. In the case of longitudinal stresses, the internal work done arises through the local  $w$  displacement and the force system is given as,

$$F = \int_A \sigma_x w \, dA \quad (75)$$

Substituting equation (39) and letting  $\delta = 1$ ,  $\xi' = -1$ ,  $\eta' = -1$ , and  $\phi' = -1$  respectively, the four generalized force components of  $F$  become,

$$N = \int_A \sigma_x \, dA \quad (76)$$

$$M_z = \int_A \sigma_x y \, dA \quad (77)$$

$$M_y = \int_A \sigma_x z \, dA \quad (78)$$

$$M_\omega = \int_A \sigma_x \omega \, dA \quad (79)$$

The first three quantities are recognized as the normal force and the bending moments acting on the cross-section. The fourth quantity is specifically related to the warping and is called the bimoment. Although it represents a real state of stress, it results in no net body force since, from equation (63), the axial warping stress distribution is seen to be exactly that of the principal sectorial coordinate which is skew symmetrical. This stress will therefore have no influence on the global equilibrium of the complete beam. For this reason, the bimoment is often referred to as a self-balancing generalized force system.

Substituting the expressions for  $\sigma$  from equation (41) into equation (76) and using the orthogonality conditions of equations (63) and (65), equation (41) can be rewritten as,

$$\sigma_x = \frac{N}{A} - \frac{M_y}{I_z}y + \frac{M_z}{I_y}z + \frac{M_\omega}{I_{\omega\omega}}\omega \quad (80)$$

The same procedure can be followed to define the generalized forces that correspond to the shear stress  $\tau$ . This stress acts along the displacement  $u$ , given by equation (31). We define:

$$Q_y = \int_A q \, dy \quad (81)$$

$$Q_z = \int_A q \, dz \quad (82)$$

$$T_w = \int_A q \, d\omega \quad (83)$$

For the case of transverse loading only,  $\delta'' = 0$ , and after substitution of equation (44) into (81), equation (41) can be written as,

$$q = -\left(\frac{Q_y}{I_z} \overline{S_y} + \frac{Q_z}{I_y} \overline{S_z} + \frac{T_w}{I_{\omega\omega}} \overline{S_\omega}\right) \quad (84)$$

where,

$$T_w = -EI_{\omega\omega}\phi''' \quad (85)$$

$$Q_y = -EI_z\xi''' \quad (86)$$

$$Q_z = -EI_y\eta''' \quad (87)$$

This expresses the total shear flow in the wall in terms of the applied loads and generalized cross-sectional properties analogous to that of traditional beam flexure theo.  $j$ . The warping torsional moment  $T_w$  characterizes the effect of the secondary shear stress distribution on the cross-section, and its magnitude reflects the relative warping stiffness of the section. Equation (74) can then be written as,

$$T = T_s + T_w = GI_t\phi' - EI_{\omega\omega}\phi''' \quad (88)$$

The total applied torsional moment is thus the sum of the St-Venant and the warping torsional moments, and at each section, there is a specific distribution of  $T_s$  and  $T_w$  dependent on the relative St-Venant and warping stiffness.

Equations (71)-(74) are the differential equations of equilibrium to be solved for a prismatic open section. For the torsional equation, a unique solution can be obtained for a beam of length  $l$  in the general form,

$$\phi(x) = C_1 + C_2x + C_3 \sinh\left(\frac{kx}{l}\right) + C_4 \cosh\left(\frac{kx}{l}\right) + P(x) \quad (89)$$

where  $P(x)$  is any particular solution and the parameter  $k$  is defined as,

$$k = l \sqrt{\frac{GI_t}{EI_{\omega\omega}}} \quad (90)$$

The coefficients of the general solution are determined from the application of the appropriate boundary conditions (See Appendix A). Once the distribution of  $\phi(x)$  is known, sectional stresses can be calculated from equations (41) and (44).

### 3.3 Closed sections

In a closed, single cell system, the St-Venant shear stress can be considered constant across the wall thickness, in contrast to the open section in which the stress varies linearly with a zero mean. This non-zero mean wall stress generates a longitudinal shear deformation. Moreover, this shear deformation cannot be neglected in this case because its existence is required by the condition that the net longitudinal displacement must be zero for a complete circuit around the cell. To account for the shear deformation, assumption (3<sup>a</sup>) of section 3.2 will be reformulated:

(3<sup>b</sup>) The longitudinal shear deformation in the walls is caused by the primary shear stress only; the additional shear deformation caused by the secondary shear stress can be neglected.

Using the new assumption, equation (33) becomes,

$$\frac{\partial u}{\partial x} + \frac{\partial w}{\partial s} = \gamma_{xs} = \frac{\tau_1}{G} \quad (91)$$

For convenience, we can define,

$$\bar{\tau} = \frac{\bar{q}}{t} = \frac{\tau_1}{GI_t \phi'} \quad (92)$$

where  $\bar{\tau}$  is then the St-Venant shear stress for a unit St-Venant torsional moment. Using this definition, and noting that the shear strain  $\gamma_{xs}$  always opposes the kinematic rotation, equation (35) can be written,

$$\frac{\partial u}{\partial x} ds = -\xi'(x) \cos \alpha(s) ds - \eta'(x) \sin \alpha(s) ds + \phi'(x)(h(s) - \frac{\bar{q}}{t} I_t) ds \quad (93)$$

For a given cross-section, the term  $\frac{\bar{q}}{t} I_t$  is well-defined and depends only on the geometry of the section. It is possible to include directly the results of the previous section if the

sectorial coordinate is expressed in the more general formulation,

$$\omega(s) = \int_0^s (h(s) - \frac{\bar{q}}{t} I_t) ds \quad (94)$$

which reduces to equation (38) for an open section since  $\bar{q}$  is then zero. Equation (94) is more properly written as the sum of two terms,

$$\omega(s) = \int_0^s h(s) ds - \int_0^s \frac{\bar{q}}{t} I_t ds \quad (95)$$

since, in fact,  $h(s)$  is a scalar quantity while  $\frac{\bar{q}}{t} I_t$  is a vector tangent to the  $s$ -coordinate but not necessarily in the same direction. Here again, the positive direction of the  $s$ -coordinate gives a counterclockwise rotation of the mobile radius vector with respect to the pole. The positive sign of the unit St-Venant shear flow is taken as counterclockwise around the cell. Written thus, the expression for the longitudinal displacement  $w(x, s)$  from equation (39), remains unchanged, and the formulation of the expressions for the principal sectorial coordinate and the axial stress is exactly as outlined in the previous section.

For a closed section, the net warping around a closed path must be zero,

$$\oint dw = 0 \quad (96)$$

It is important to check that this requirement is embodied in assumption (3<sup>b</sup>). For the sake of clarity, consider the case of pure torsion. We have, for a closed section, from equation (15)

$$T_s = G I_t \phi' = \oint q_1 h ds \quad (97)$$

where,

$$I_t = \frac{4A}{\oint \frac{ds}{t}} \quad (98)$$

hence,

$$q_1 = \frac{2A\phi'G}{\oint \frac{ds}{t}} \quad (99)$$

Recalling the definition of  $\bar{q}$ , we have,

$$\oint \frac{\bar{q}}{t} I_t \phi' ds = 2A\phi' \quad (100)$$

or, equivalently,

$$\oint \frac{\bar{q}}{t} I_t \phi' ds = \phi' \oint h(s) ds \quad (101)$$

which is exactly satisfied by enforcing equation (96), using the definition of the sectorial coordinate of equation (95).

For the closed section, the starting point for the integration of equation (43) can no longer be a free edge and the constant of integration cannot be taken as zero. However, this constant can be found in the following manner. Again, for simplicity, consider pure torsion. The secondary shear flow is then,

$$q_2(x, s) = E(\phi'''(x)\bar{S}_\omega(s)) + (q_2)_0 \quad (102)$$

An arbitrary starting point can be chosen for the integration of  $\bar{S}_\omega(s)$  to find the first term. This is equivalent to cutting the cell open at this point and finding the corresponding shear distribution of the 'open' section. We define,

$$q_2(x, s) = q_2^* + (q_2)_0 \quad (103)$$

where the  $(q_2)_0$  is a constant correction factor. According to assumption (3<sup>b</sup>), the longitudinal shear strain caused by the secondary shear flow is negligible. In support of this assumption, it is consistent to determine the constant shear flows in such a manner that  $q_2$  gives no contribution to the shear deformation of the cell,

$$\oint \gamma_2 ds = \oint \frac{q_2}{Gt} ds = 0 \quad (104)$$

Substituting equation (104),

$$(q_2)_0 = -\frac{\oint \frac{q_2^*}{t} ds}{\oint \frac{ds}{t}} \quad (105)$$

hence the complete shear distribution in the cell can be found once  $(q_2)_0$  is calculated.

The warping torsional moment is,

$$T_w = \oint q_2 h ds = \oint (q_2^* + (q_2)_0) h ds \quad (106)$$

According to equation (94),

$$h(s) ds = d\omega + \frac{\bar{q}}{t} I_t ds \quad (107)$$

substituting into equation (106),

$$T_w = \oint (q_2^* + (q_2)_0) d\omega + \oint [(q_2^* + (q_2)_0) \frac{\bar{q}}{t} I_t] ds \quad (108)$$

The second integral is zero from equation (104). Performing the integration on the line integral of  $s$  by parts gives, for the first term,

$$\oint (q_2^* + (q_2)_0) \frac{\partial \omega}{\partial s} ds = [(q_2^* + (q_2)_0) \omega]_A - \oint \omega \frac{\partial}{\partial s} (q_2^* + (q_2)_0) \quad (109)$$

Since the integration is performed for a complete path, the first term on the right is zero. The constant correction shear flow  $(q_2)_0$  can be dropped as it is constant, leaving,

$$T_w = - \oint \omega \frac{\partial}{\partial s} q_2 = -E\phi''' \oint \omega^2 t ds = -EI_{\omega\omega}\phi''' \quad (110)$$

By comparing this expression with equation (87), we see that the expression for the warping torsional moment is unchanged. The differential equation is then, as before,

$$T = T_s + T_w \quad (111)$$

$$T = GI_t\phi' - EI_{\omega\omega}\phi''' \quad (112)$$

with the value of  $I_t$  and  $I_{\omega\omega}$  as appropriate for the closed cell, and the same general hyperbolic solution form is obtained. Once known, the distribution of  $\phi$  and its derivatives can be used to scale the sectional shear and axial stresses, where these distributions are given for the case of pure torsion as,

$$q_{total} = \frac{GI_t}{2A}\phi' + E\phi'''\overline{S}_\omega(s) + (q_2)_0 \quad (113)$$

and,

$$\sigma_x = -E\phi'' \left[ \int_0^s h(s) ds - \int_0^s \frac{\bar{q}}{t} I_t ds \right] \quad (114)$$

### 3.4 Multi-cell sections

Multi-cell sections can be treated as a generalization of the theory for a single cell cross-section, and the development leads to the same differential equation. The sectorial coordinate is again given by,

$$\omega(s) = \int_0^s (h - \frac{\bar{q}}{t} I_t) ds \quad (115)$$

In this case, for a given cell wall, the unit shear flow  $\bar{q}$  is the algebraic sum of the constant St-Venant unit shear flows corresponding to each cell of which it is part. Here again, a consistent sign convention must be observed. Once the principal sectorial coordinate is defined for the cross-section, all of the relevant properties can be calculated exactly as discussed in the previous sections.

To find the stress distribution in a multi-cell section,  $nc$  constants of integration must be found, where  $nc$  is the number of cells in the section. The requirement of zero net secondary shear strain is enforced for each cell. In terms of stress, this gives,

$$\oint_i q_2 \frac{ds}{t} = 0 \quad i = 1, nc \quad (116)$$

This allows the formation of a matrix system, the solution of which gives the required  $(q_2)_0$  correcting factor for each cell. Using the same notation as in section 3.3, we can develop for cell  $i$ ,

$$\oint_i q_2^* \frac{ds}{t} + (q_2)_{0,i} \oint \frac{ds}{t} - (q_2)_{0,j} \oint_{ij} \frac{ds}{t} - \dots = 0 \quad (117)$$

where  $q_2^*$  is again the shear flow distribution derived from equation (103) after cutting the cells open. In matrix form, equation (117) can be written,

$$[\kappa] ((q_2)_0) = (q_2^*) \quad (118)$$

where it can be seen that the  $\kappa$  coefficient matrix is exactly that derived for the solution of the St-Venant shear flows.

Solving for the  $(q_2)_0$ , the warping secondary shear stress can be found from equation (113) and the axial stress distribution from equation (114). The total shear stress distribution is the sum of the St-Venant, transverse, and secondary warping shear stress distributions. The longitudinal stress distribution is given by the sum of the two bending and the axial stress distributions.

### 3.5 A Refined Beam Torsion Model

The development of the previous beam torsional model has been consistent with most classical beam theory, wherein equilibrium is enforced despite the neglect of secondary shear deformations. This leads to the assumption that the warping deformation is proportional to the twist, as in the case of unrestrained warping. A more general form of warping distribution has been proposed<sup>(1)</sup> in which a displacement field proportional to the sectorial coordinate, but independent of the twist, is assumed. This new degree of freedom is commonly called the generalized warping function. Unfortunately, such an assumption can lead to unsatisfactory local equilibrium conditions, and the warping stress distributions predicted by this theory are not completely reliable;<sup>(13)</sup> however, the sectional loads calculated from the refined theory can be used in the classical stress equations to improve the stress prediction accuracy of that model.

For simplicity, consider the case of pure torsion. Since no assumption is made about the shear deformation in the  $x - s$  plane, Figure 6, equation (91) is,

$$\frac{\partial u}{\partial x} + \frac{\partial w}{\partial s} = \gamma_{xs} \quad (119)$$

The expression for the tangential displacement  $u$  remains unchanged as the assumption of no in-plane distortion of the section is retained. For pure torsion, we have from equation (31),

$$u(x, s) = \phi(x)h(s) \quad (120)$$

The longitudinal displacement  $w$  will again be assumed proportional to the sectorial coordinate and to an arbitrary function of the longitudinal position  $x$ , rather than the twist  $\phi'$ ,

$$w(x, s) = -\theta(x)\omega(s) \quad (121)$$

where  $\theta(x)$  is defined as the generalized warping function. The negative sign is introduced to retain the similarity with the previous development. Substituting equations (120) and (121) into equation (119) gives the shear deformation as,

$$\gamma_{zs} = \phi' h(s) - \theta(x)\dot{\omega}(s) \quad (122)$$

where the overdot indicates differentiation with respect to  $s$ ,

$$\dot{\omega}(s) = \frac{\partial \omega}{\partial s} = h(s) - \frac{\bar{q} I_t}{t}$$

The stresses can then be expressed as,

$$\sigma(x, s) = E \frac{\partial w}{\partial x} = -E\theta'(x)\omega(s) \quad (123)$$

$$\tau(x, s) = G\gamma_{zs} = G(\phi' h(s) - \theta(x)\dot{\omega}(s)) \quad (124)$$

where  $\tau$  now represents the complete shear stress in the cross-section derived from an assumed displacement field. The shear center location is not affected by these new assumptions, and can be found in the same manner as previously discussed. The total torque on the cross-section is,

$$T = \int h(s)\tau(x, s)t ds \quad (125)$$

Substituting from equations (122) and (123), and using the relation,

$$\int \bar{\tau} I_t h t ds = \int \frac{\bar{q} h}{G\phi'} ds = \sum_{i=1}^{nc} \frac{2q_i A_i}{G\phi'} = I_t \quad (126)$$

we have a differential equation in  $\phi$  and  $\theta$ ,

$$T = G I_{hh} \phi'(x) - G(I_{hh} - I_t)\theta \quad (127)$$

or, more generally,

$$G I_{hh} \phi'' - G(I_{hh} - I_t)\theta' + m = 0 \quad (128)$$

where,

$$m = -\frac{\partial T}{\partial x}$$

and,

$$I_{hh} = \int h^2 t ds \quad (129)$$

is called the central moment of area. Strictly, equation (126) is valid if only the closed cell contributions are important in the calculation of the St-Venant modulus. This is an acceptable assumption for most ship hull analyses, but will introduce inaccuracy in the analysis of predominantly open configurations.

The differential equation contains two unknown functions  $\theta(x)$  and  $\phi(x)$ , and another relationship is required before a solution is possible. The principle of virtual work can be used to establish a further relationship between  $\theta(x)$  and  $\phi(x)$  based on the assumption of axial equilibrium. Away from local end effects, the internal virtual work of the shear stresses can be equated to the work done by the external forces moving through a virtual displacement field. The incremental axial stress in this case can be considered as the external load, Figure 10. In the general case, this stress will also include the contributions from bending and longitudinal loads. We can write, for a unit  $\theta$ ,

$$\int \int \frac{\partial \sigma}{\partial x} \tilde{w} t ds dx = \int \int \tau \tilde{\gamma} t ds dx \quad (130)$$

where  $\tilde{w}$  and  $\tilde{\gamma}$  represent virtual displacement and strain fields respectively. Using equation (123) in (130), we have, after substitution and cancelation,

$$E\theta''(x) \int \omega^2 t ds + G\phi'(x) \int h\omega t ds - G\theta \int \dot{\omega}^2 t ds = 0 \quad (131)$$

Expanding the second integral, we obtain,

$$\int h\omega t ds = \int h(h - \frac{\bar{q}}{tI_t})t ds = I_{hh} - I_t \quad (132)$$

and the third integral becomes,

$$\int \dot{\omega}^2 t ds = \int (h - \frac{\bar{q}}{tI_t})^2 t ds = I_{hh} - 2I_t + \int (\frac{\bar{q}}{tI_t})^2 t ds \quad (133)$$

Evaluating the final integral,

$$\int (\frac{\bar{q}}{tI_t})^2 t ds = \int \bar{q} ds \int \bar{\tau} ds = \sum_{i=1}^{nc} (\bar{q}_i \oint \frac{\bar{q}}{t} ds) \quad (134)$$

which leads to,

$$\sum_{i=1}^{nc} (\frac{\bar{q}_i}{G\phi'} \oint \frac{q}{t} ds) = 2 \sum_{i=1}^{nc} A_i q_i = I_t \quad (135)$$

where it is again assumed that the open section contribution to  $I_t$  is negligible. Equation (131) can then be written,

$$EI_{\omega\omega}\theta'' + G(\phi' - \theta)(I_{hh} - I_t) = 0 \quad (136)$$

Solving equation (128) for  $\theta'$ ,

$$\theta' = \frac{m + GI_{hh}\phi''}{G(I_{hh} - I_t)} \quad (137)$$

After appropriate differentiation and substitution,  $\theta$  and its derivatives can be eliminated from equation (136) to give,

$$EI_{\omega\omega\rho}\phi'''' - GI_t\phi'' = m - \frac{E\rho I_{\omega\omega}m''}{GI_{hh}} \quad (138)$$

where,

$$\rho = \frac{I_{hh}}{I_{hh} - I_t} \quad (139)$$

The analytical solution of this differential equation can be difficult if the applied moment distribution is of higher than linear order. In practise, linear or harmonic variations can be used to model moment distributions on ship hulls, in which case the particular solution of equation (137) is usually evident. The characteristic solution is given as in equation (89). The warping factor  $\theta$  can be obtained, after solution of the differential equation, from equations (137) and (138),

$$\theta = \phi' + \frac{EI_{\omega\omega}}{G^2} \frac{(m' + GI_{hh}\phi''')}{(I_{hh} - I_t)^2} \quad (140)$$

As is evident from equation (140), the warping displacement is now a function not only of the twist, as in free torsion, but also is dependent on the warping stiffness properties and the loading distribution on the beam. The total torque can be found from substitution of equation (140) into equation (128) to obtain,

$$T = GI_t\phi' - EI_{\omega\omega\rho}\phi'''' - \frac{EI_{\omega\omega\rho}}{GI_{hh}}m' \quad (141)$$

or,

$$T = T_s + T_w \quad (142)$$

where, as before,

$$T_s = GI_t\phi' \quad (143)$$

and,

$$T_w = -EI_{\omega\omega\rho}\phi'''' - \frac{EI_{\omega\omega\rho}}{GI_{hh}}m' \quad (144)$$

Recalling the definition of the bimoment from equation (76), and using equation (138),

$$M_\omega = - \int \sigma \omega t ds = -E \int \frac{\partial \theta(x)}{\partial x} \omega^2 t ds \quad (145)$$

or,

$$M_\omega = - \left[ \frac{EI_{\omega\omega}}{G(I_{hh} - I_t)} + EI_{\omega\omega} \phi'' \rho \right] \quad (146)$$

After solution of the differential equation and calculation of the internal forces  $T_s$ ,  $T_w$  and  $M_\omega$ , the stresses can be calculated from equation (123). This gives,

$$\tau(x, s) = G \phi' \bar{\tau} - \frac{EI_{\omega\omega} \dot{\omega}}{(I_{hh} - I_t)^2} \left[ I_{hh} \phi''' + \frac{m'}{G} \right] \quad (147)$$

and,

$$\sigma(x, s) = E \left[ \frac{m + GI_{hh} \phi''}{G(I_{hh} - I_t)} \right] \omega(s) \quad (148)$$

In general, this procedure does not provide an equilibrium stress system at all points, since the formulation is based on an assumed displacement field, and the equilibrium statement,

$$\frac{\partial(t\sigma)}{\partial x} + \frac{\partial(t\tau)}{\partial s} = 0 \quad (149)$$

is not necessarily satisfied. For example, on a single cell cross-section of constant thickness, with  $m = m' = 0$ , the equilibrium statement leads to,

$$\omega(s) - \frac{I_{\omega\omega}}{(I_{hh} - I_t)} \dot{\omega}(s) \neq 0 \quad (150)$$

This deficiency is particularly severe in the case of sections which are predominately open, since the assumption of negligible open section contribution to  $I_t$  becomes less acceptable. It is recommended in such cases that the stresses be calculated from the theory discussed in the previous section, using the forces derived from the refined model.

### 3.6 Account of Shear Deformation

Each of the three assumptions outlined in the development of the beam theory introduces some error into the method. Of particular concern are the assumption of no cross-sectional distortion and the neglect of the warping shear deformation. The former cannot be relaxed within the limits of the sectorially based thin-walled beam theories which depend on an invariant geometry; however, it is, in principle, possible to include the effects of the shear

deformation if an iterative calculation method is used. The simplest method typically uses the warping moment from an initial solution neglecting the shear strains to define a warping stress distribution. The cross-sectional properties are then recalculated, this process continuing until a prescribed convergence criterion is satisfied. As an example, this approach can be developed in conjunction with the refined beam theory of the previous section. The equilibrium condition becomes,

$$\frac{\partial u}{\partial x} + \frac{\partial w}{\partial s} = \frac{\tau_1 + \tau_2}{G} \quad (151)$$

and the principal sectorial coordinate becomes,

$$\omega(s) = \int_0^s h \, ds - \int_0^s \bar{\tau}_1 + \bar{\tau}_2 \, ds \quad (152)$$

where  $\bar{\tau}_2$  is the initially unknown warping shear stress distribution function. The St-Venant shear stress function  $\bar{\tau}$  (here called  $\bar{\tau}_1$  for clarity) was defined as,

$$\bar{\tau}_1 = \frac{\tau_1}{I_t G \phi'} \quad (153)$$

Since  $\tau_1$  is proportional to  $\phi'$ , this function is independent of the loading. The warping shear stress function could be defined in a similar fashion as,

$$\bar{\tau}_2 = \frac{\tau_2}{G \theta} \quad (154)$$

and if  $\tau_2$  were proportional to  $\theta$ , this distribution function would also be independent of the load. With reference to equation (147), it can be seen that a simple proportionality with  $\theta$  does not exist, and in fact a more relevant divisor might be  $\phi'''$ . However, because the shear stress distribution of the refined method generally does not provide equilibrium, it is more common to use the original warping torsion shear stress distribution given by,

$$\tau_2 = -\frac{T_w \bar{S}_w}{I_{\omega} t} \quad (155)$$

with  $T_w$  derived from the refined theory. This formulation leads to a solution uniquely defined by the load and boundary conditions, which invalidates any superposition of different solutions. From the results described by Westin<sup>(2)</sup>, it appears that this iterative procedure is not always convergent, particularly if large warping shear stresses are present, as will occur at a warping restraint. In applications of this method to typical ship structures, the boundary conditions may require certain idealizations to facilitate a convergent solution.

A more detailed approach to the complete inclusion of the warping shear deformations has been described by Pittaluga.<sup>(3)</sup> This method uses a more general St-Venant solution

of the equilibrium equations to define the requirements of certain cross-sectional functions. The distributions of these functions are solved by a finite strip method utilizing linear interpolation functions within the cross-section. Using fairly realistic assumptions about the loading and twist distribution, an iterative procedure yields the desired warping torsional stiffness independent of the applied load. Although there are definite approximations used in this development, convergence does not appear to be a problem.

Both of the methods outlined above can be applied to the analysis of non-prismatic beams, either by a finite beam element approach,<sup>(3)</sup> or a transfer matrix method.<sup>(2,13)</sup> An advantage of Pittaluga's method is that only one solution of the complete system is required once the various sectional properties have been calculated. The application of the thin-walled theories in the analysis of non-prismatic beams is discussed further in the following section.

In some instances, the inclusion of warping shear deformations will improve the displacement and stress predictions of the thin-walled beam methods; however, in many structures, the largest error in the theory is introduced by the assumption of no transverse distortion, and the effects of shear deformation are quite nominal. In those cases, it is questionable whether the added complexity of iterative computations are justifiable, particularly if a convergent solution is not guaranteed.

## 4 Application to Non-Prismatic Beams

### 4.1 General Approaches

The warping based theories of the behaviour of prismatic thin-walled sections described in this report yield quite accurate stress predictions for transversely rigid structures. A natural extension of the theoretical development is its application to the analysis of non-prismatic structures such as ship hulls. This generalization presents a number of difficulties; either the differential equations must be reformulated to account for the longitudinal variation of cross-sectional properties, or the structure must be approximated by prismatic discretization. The former method yields a more complex system of differential equations, and neither method provides complete internal stress equilibrium. Despite these drawbacks, the prismatic beam theory is often used in the analysis of non-prismatic beams, and a variety of methods have been presented in the literature.<sup>(2,3,4,13,14,15)</sup>

The simplest application of the theory is to assume that the hull girder behaves as a prismatic beam having some longitudinally averaged characteristics. Such a method can provide boundary conditions for more detailed internal analyses, but in general does not yield accurate local stress predictions.

A second alternative is to model the hull as a series of prismatic segments, using the finite beam or transfer matrix methods to assemble the complete representation of the hull. In the

finite beam method, interpolation functions are formed to describe the internal deformation distributions in terms of the local nodal degrees of freedom. Using the principle of virtual work, the nodal degrees of freedom are related to the generalized force vector, defining the beam element stiffness matrix. Various choices of deformation and interpolation functions lead to alternative element stiffness representations.<sup>(3,15,16)</sup> The element stiffnesses and loads are assembled in the usual manner to obtain the overall system of equilibrium equations, and application of suitable constraints on the system allows a solution via normal matrix methods. The transfer matrix method also results in a global representation of the complete beam as an assembly of individual transfer matrices which link displacements at either end of a beam segment. In this case, the actual differential equation defines the deformations in each prismatic segment. The system of equations is solved for the beam end displacements (or loads) which comply with the boundary conditions.

An unavoidable deficiency is the inability of either approach to correctly describe the compatibility of warping displacements at the model geometric discontinuities. As a result, complete internal equilibrium is not maintained, and the stress estimates from these models are least accurate precisely at the locations where good predictions are most valuable. A number of methods of minimizing the compatibility errors at discontinuities have been proposed, such as a least squares minimization of the displacement gap field between the segments,<sup>(16)</sup> or the application of orthogonality criteria to partially satisfy the internal equilibrium requirements.<sup>(4,13)</sup> For ship hull sections which have only one plane of symmetry, improved compatibility can also be obtained by maintaining the coupling between the horizontal bending and torsional displacements at a discontinuity via coupling coefficients.

A further refinement in the modelling of non-prismatic structures is the generalization of the differential equations of equilibrium to include the longitudinal variation of sectional properties. This leads in the most general case to an impractically complex set of coupled differential equations with longitudinal properties which cannot be calculated by conventional cross-sectional analysis programs. If suitable assumptions are made of the relative magnitudes of the variations of the structural properties and displacements, this approach can be reduced to a tenable format. The effects of transverse beams, torsion boxes and other internal torsional restraints can be included in both this approach and the discretization methods by the introduction of equivalent bimoment springs and distributed loading.

#### 4.2 A Flexural-Torsional Model

As an example of the generalization and application of the prismatic beam theory to the analysis of non-prismatic structures, a method of flexural-torsional analysis is presented. This method models the ship as a beam with slowly varying cross-sectional properties, an assumption which possibly allows the neglect of the longitudinal variation characteristics, although a verification of this assumption remains to be ascertained. For the flexural-

torsional problem, this approach yields a boundary value problem of four coupled differential equations in the generalized displacements  $\phi, \theta, \xi, \beta$ . This theory has been developed and implemented in a computer program<sup>(4,7,17)</sup> which is currently in use at DREA as a part of the ship hull torsional analysis program suite. The analysis considers only horizontal flexure, since, for ship hulls which normally possess center-plane symmetry, the vertical flexure and torsional response are independent and the former can be obtained by other methods.

An energy variational approach can be used to determine the equations of motion of the beam,

$$\delta \int_{t_1}^{t_2} (T - (U + W)) dt = 0 \quad (156)$$

where  $\delta$  is the first variation with respect to time and  $T, U, W$  are the kinetic, internal and external energies of the system respectively. To evaluate the energy expressions for a beam in which the location of the principal axes and shear center are longitudinally varying, a fixed baseline must be established for the coordinate system, Figure 12. From equation (39), we have, considering only horizontal bending,

$$w(x, s) = -\beta(x)y(s) - \theta(x)\omega(x, s) \quad (157)$$

where the warping function of section 3.5 has replaced  $\phi'$ , and  $\beta = \xi'$ . The tangential displacement reflects the influence of the new coordinate system,

$$u(x, s) = \phi(x)h(s) + (\xi(x) - z_s\phi(x))\frac{dy}{ds} \quad (158)$$

where  $z_s$  is the offset of the shear center from the baseline. Formulating the strains in accordance with the assumptions previously discussed, we have,

$$\epsilon_x = \frac{\partial w}{\partial x} \quad (159)$$

$$\gamma_{xs} = \frac{\partial w}{\partial s} + \frac{\partial u}{\partial x} \quad (160)$$

The internal strain energy of the system is,

$$U = \frac{1}{2} \int_0^l \int_A (E\epsilon_x^2 + G\gamma_{xs}^2) dA dx \quad (161)$$

Substituting the appropriate expressions for the strains, we can obtain an expression for the total internal strain energy in terms of the four generalized coordinates and their derivatives. To simplify this expression, it is assumed that the longitudinal variation is slow, that is, the  $x$ -derivatives of the sectional points and sectorial coordinate can be neglected in comparison

to the corresponding derivatives of displacements. The  $s$ -coordinate origin is defined again in such a way that,

$$I_{\omega y} = I_{\omega z} = S_{\omega} = 0 \quad (162)$$

Applying these criteria, and recalling the relations of equations (132) and (134), the strain energy becomes,

$$U = \frac{1}{2} \int_0^l [E\theta'^2 I_{\omega\omega} + \beta'^2 I_z] \quad (163)$$

$$+ \frac{1}{2} \int_0^l G[\phi'^2 I_{hh} + (\theta^2 - 2\phi'\theta)(I_{hh} - I_t)] \quad (164)$$

$$+ 2I_{ph}(\theta\beta + \theta(z_s\phi)' - \theta\xi' - \phi'(z_s\phi)' - \phi'\beta + \phi'\xi') \quad (165)$$

$$+ I_{pp}(\xi'^2 + (z_s\phi)'^2 + \beta^2 - 2\xi'(z_s\phi)' - 2\xi'\beta + 2(z_s\phi)'\beta)] dx \quad (166)$$

The prime and dot superscripts again denote differentiation with respect to  $x$  and  $s$  respectively.

The potential energy of the loads for the system can be expressed as,

$$W = - \int_0^l (p_y \xi + (m_x + p_y z_s)\phi + m_x \beta) dx \quad (167)$$

If we consider only the static problem, the above energy expressions can be substituted into equation (156) and the variation taken with respect to each of the displacement variables  $\beta, \phi', \xi, \theta$ . This yields the following four coupled differential equations of static equilibrium,

$$[EI_z \beta']' + GI_{pp}(\xi' - \beta - (z_s\phi)') + GI_{ph}(\phi' - \theta) = -m_x \quad (168)$$

$$[GI_{pp}(\xi' - (z_s\phi)' - \beta) + GI_{ph}(\phi' - \theta)]' = -p_y \quad (169)$$

$$[GI_{hh}\phi' - G\theta(I_{hh} - I_t) + GI_{ph}(\xi' - (z_s\phi)' - \beta)]' = -m_x - p_y z_s \quad (170)$$

$$[EI_{\omega\omega}\theta']' + GI_{ph}(\beta - \xi' - (z_s\phi)') + G(\theta - \phi')(I_{hh} - I_t) = 0 \quad (171)$$

For a dynamic analysis, the kinetic energy and time variation of the system is included in the functional and the variation procedure yields the equations of motion of the system. Note that, in the most general case of an analysis of a beam, this procedure will yield seven coupled differential equations, rather than four, since the axial, and vertical bending and displacement variables will also be included (See Reference 16).

The boundary value problem in the present case requires eight boundary conditions for solution. These can be defined in terms of displacements or forces; forces are used

here. Since this program has been developed specifically for the analysis of ship hulls, the horizontal bending moment, torsional moment and shear force are assumed to be zero at each end. Following Reference 4, the bimoment, rather than assumed zero, can be assigned a value to reflect the different forms of warping restraint which can occur at the ends of a hull,

$$M_{\omega} = k\theta|_{x=0 \ x=l} = 0 \quad (172)$$

or

$$[EI_{\omega\omega}\theta' + k\theta]_{x=0 \ x=l} = 0 \quad (173)$$

Abrupt changes in cross-section can be incorporated in this formulation as discontinuity conditions analogous to boundary conditions. In the real beam, these geometric discontinuities cause finite but often non-localized stress gradients. In the numerical model, they are two dimensional phenomena which result in an axial displacement gap field at the junction of the sections. If we assume that the discontinuity is effectively closed with a stress distribution proportional to the gap size, an assumption consistent with linear behaviour, then minimization of this stress field in some way may yield a good approximation to the true stress distribution.

A relatively simple method can be developed if it is assumed that sections spanning a discontinuity can undergo only rigid body motion with respect to to each other. This results in two relationships between the displacements on either side of a discontinuity at  $x_i$ ,

$$\theta(x_i^+) = \alpha_1^i \theta(x_i^-) \quad (174)$$

$$\beta(x_i^+) = \beta(x_i^-) + \alpha_2^i \theta(x_i^-) \quad (175)$$

where the  $\alpha^i$  are discontinuity coefficients to be determined in some consistent manner. The axial displacements are then,

$$w(x_i^-, s) = -\beta(x_i^-)y(s) - \theta(x_i^-)\omega(x_i^-, s) \quad (176)$$

$$w(x_i^+, s) = -\beta(x_i^-)y(s) - \theta(x_i^-)(\alpha_1^i\omega(x_i^+, s) + \alpha_2^i y(s)) \quad (177)$$

and, in accordance with the above assumption, the differential stress field at the discontinuity is described by,

$$\Delta\sigma_x = c(w(x_i^+) - w(x_i^-)) \quad (178)$$

where  $c$  is a constant. To determine the values of the two discontinuity coefficients which may minimize the effect of the incompatibility, it is consistent to apply local equilibrium conditions to the differential stress field. For complete equilibrium, these requirements are,

$$\int_A \Delta\sigma_x (w(x_i^-) + w(x_i^+)) dA = 0 \quad (179)$$

$$\int_A \Delta \sigma_z dA = 0 \quad (180)$$

$$\int_A \Delta \sigma_{zy} dA = 0 \quad (181)$$

The first expression is the equilibrium statement for the bimoment at the section, and the second and third integrals refer to the axial and horizontal bending equilibrium respectively. Two of these conditions can be satisfied with the two degrees of freedom available from the rigid body motion assumption. In the current formulation these are chosen as the bimoment and horizontal bending relations. (These criteria can be satisfied identically in certain cases of complete cross-sectional symmetry; in the more general case, the application of the simple rigid body parameters will not completely alleviate the incompatibility.) Substituting equations (176) and (178) into (179), the coefficients  $\alpha_1^i$  and  $\alpha_2^i$  can be found in terms of the sectional properties at the discontinuity,

$$\alpha_1^i = \sqrt{\frac{I_{yy}^- I_{\omega\omega}^- - I_{y\omega}^-^2}{I_{yy}^+ I_{\omega\omega}^+ - I_{y\omega}^+^2}} \quad (182)$$

$$\alpha_2^i = \frac{I_{y\omega}^- - \alpha_1^i I_{y\omega}^+}{I_{yy}^-} \quad (183)$$

The cross-sectional properties in these expressions are calculated for the cross-section which is common to both sides of the discontinuity. Since the coefficients are functions of two cross-sections, their values cannot be established in a single cross-sectional property computation. The calculation of these compatibility coefficients is discussed in more detail in Reference 20.

The necessary relations between the loads at the discontinuities can be derived from the requirement of overall internal equilibrium at the discontinuity, which implies equality of the virtual work done by the stress field under a virtual displacement,

$$\int_{A_{z_i^-}} \sigma_z \tilde{w} dA = \int_{A_{z_i^+}} \sigma_z \tilde{w} dA \quad (184)$$

Using the expressions of equations (176) for  $w$ , this yields,

$$M_z(x_i^+) = M_z(x_i^-) \quad (185)$$

$$M_\omega(x_i^+) = \frac{1}{\alpha_1^i} (M_\omega(x_i^-) + \alpha_2^i M_z(x_i^-)) \quad (186)$$

The horizontal shear force is continuous across the discontinuity as is the rotation and horizontal displacement,

$$P_y(x_i^+) = P_y(x_i^-) \quad (187)$$

$$\phi(x_i^+) = \phi(x_i^-) \quad (188)$$

$$\xi(x_i^+) = \xi(x_i^-) \quad (189)$$

and the torsional moment relation becomes,

$$T(x_i^+) = T(x_i^-) + P_v(z_s(x_i^+) - z_s(x_i^-)) \quad (190)$$

because of the difference in shear center locations.

The warping restraint of internal structures such as torsion boxes and deck strips across large openings can be included in the analysis by their introduction as point bimoment springs in the system in the form,

$$M_\omega(x_i^+) - M_\omega(x_i^-) = K_\omega^i \theta(x_i) \quad (191)$$

The warping stiffness  $K_\omega^i$  expresses the restraining effect of the structure as a function of the end fixity, torsional and bending stiffness, and sectorial coordinate of a general point of attachment of the internal structure. The inclusion of larger restraining structures such as wide deck strips can be derived in terms of distributed contributions to all forces and is included directly in the right hand side of the differential equations (168)-(171). A full development of the stiffness derivation of internal structures and the modifications required in the differential equations can be found in Reference 4.

The discussion of this section has presented the derivation of the differential equations of equilibrium for the flexural-torsional problem. This constitutes a special case of the more general formulation of the equations of motion, obtained from the variation of the complete energy functional. For a ship structure, a complete derivation must contain the hydrodynamic effects relevant to hull motion in the expression for the kinetic energy. In the current approach, these hydrodynamic terms are the added fluid mass associated with the sway acceleration and added mass moment of inertia. They are currently calculated on the basis of Lewis form representations of discrete hull sections.<sup>(18)</sup>

The mathematics of the solution of the complete boundary value problem is quite involved and is beyond the scope of this report. The method involves the choice of a set of separable functions for the generalized displacements in the form,

$$[D] = [X_e] \sin(\Omega t + \Psi) \quad (192)$$

where  $D$  is the vector of generalized displacements,  $X_e$  is a vector of arbitrary, integrable functions, and  $\Omega$  and  $\Psi$  are the frequency and phase angle respectively. The substitution of the form (192) into the differential equations (168)-(171) and boundary and discontinuity conditions yields a self-adjoint, positive semi-definite eigenvalue problem which can be solved by an iterative approximation technique. For the calculation of natural frequencies, the iteration vectors must be normalized and orthogonalized at each iteration and a solution

is established when successive eigenvector norms differ by an arbitrary small number. The response to periodic forcing functions is expressed as a series summation of the modal responses derived by the iteration process.

The solution method originally supplied by Pedersen has been adapted for use at DREA and provides the dynamic response predictions as above, and also the longitudinal distributions of the displacement variables relative to the baseline. The distribution of the bimoment, warping moment and St-Venant torsional moment can then be input into a suitable stress calculation program (typically the same program that generates the cross-sectional properties) to obtain the sectional stress distributions.

## 5 Implementation and Evaluation of the Flexural-Torsional Model

The theoretical basis for the torsional analysis of beams with slowly varying cross-sectional properties has been developed, and a solution method has been programmed. This section discusses the program and its application to actual structures. The displacement and stress predictions are compared to both published data and to finite element comparison solutions for several simple box beams. The beam method is then utilized in a static torsional analysis of the hull of a frigate.

### 5.1 DREA Torsional Analysis Program Suite

The torsional analysis system in use at DREA comprises three independent but compatible computer programs. Since several of these programs are of a general purpose nature this section discusses only the specific details relevant to a torsional analysis. The first program in the suite, TPGEOM, is a planar digitization program which provides the data base for each cross-section. This data base includes all plate thicknesses, beam locations and dimensions relative to a baseline which is usually defined by the keel in the case of hull sections.

The second program, SCRAP, accesses the data base and provides a general purpose cross-sectional property and strength analysis capability. This includes the calculation of the added fluid mass for a section based on the two dimensional Lewis form method, the calculation of warping related sectional properties, and graphical display of all stress distributions from specified transverse or torsional shear forces, bending moments, and bimoments. The torsional stress distributions are based on the warping torsion theory discussed in Sections 3.2, 3.3 and 3.4. SCRAP stores the relevant sectional information for use either in the flexural-torsional beam model, or in an equivalent beam format suitable for further analysis with an in-house finite element program VAST<sup>(19)</sup>. The equivalent

beam models are used for prediction of vertical hull vibration characteristics and dynamic response.

The third computer program is a Fortran transcription of the TORSON program supplied to DREA by the Department of Ocean Engineering, Technical University of Denmark. This program is based on the flexural-torsional theory presented in Section 4.2, and solves the system of equations subject to the appropriate boundary conditions, and discontinuity and internal restraint conditions. The program is currently utilized only for static stress analysis, although further capabilities may be developed in the future. For this case, the program provides longitudinal baseline distributions of the global displacements, and St-Venant moments, warping moments and bimoments for the beam, given the data file as output by SCRAP and a description of the external loads. The internal sectional loads are then used in SCRAP to scale the warping based sectional stress distributions. The St-Venant, transverse shear, and secondary shear stresses, and the bimoment and primary bending stresses can be superposed respectively to obtain the total shear and longitudinal stress distributions. Specific aspects of the operation of the torsional analysis programs are presented in Reference 20.

## 5.2 Evaluation of the torsional analysis system

A number of simple test structures have been analyzed to evaluate the displacement and stress prediction capability of the flexural-torsional method. To facilitate comparison of the results with finite element solutions, these models have been prismatic beams with simple geometric discontinuities.

Because the TORSON program has been transcribed into Fortran computer code from its original Hewlett Packard Basic form, it was first necessary to run a sample problem for which results are available from the author to ensure that the program integrity had been maintained. A comparison with the available results for the beam of Figure 13 is presented in Figures 14 and 15. These figures indicate that the SCRAP and TORSON programs are providing results in complete agreement with those of Pedersen. A finite element comparison solution provided by Pedersen is also shown. There is very good agreement in the rotation angle predictions, and the axial stresses are in general agreement except very close to the discontinuity.

As an independent evaluation, a second test structure with an intermediate deck and a smaller deck opening has been studied, as this beam characterizes an actual ship structure somewhat better than the first model. A detailed finite element model of one half of the beam has been used as a comparison solution. This model, shown in Figure 16, comprised 885 nodes, 270 isoparametric shell elements, and 30 isoparametric membrane elements. Symmetry boundary conditions were used and longitudinal restraints were imposed at points of zero warping predicted by the SCRAP cross-sectional analysis. An end moment was

imposed as an antisymmetric series of point loads at the free end of the beam. The initial comparison of the results from an unstiffened finite element model with those of the flexural-torsional beam method were very poor. A series of other models were analyzed with similar results; the finite element solutions predicted much larger values of rotation and stress than both the classical and beam theory methods. An investigation of this disparity<sup>(21)</sup> indicated that there were large cross-sectional distortions occurring which are not accounted for in either the traditional St-Venant or the flexural-torsional theory. These distortions give rise to high plate bending stresses and large rotational displacements. The disparity between the solutions also appeared sensitive to the tendency of the structure to warp, a characteristic not always known a priori.

To reduce the in-plane distortion, and hence better approximate the assumption inherent in the beam theory, the internal transverse membranes evident in Figure 16 were introduced into the finite element model. The twist angle and axial stress comparisons for that model are presented in Figures 17 and 18 respectively. The twist angle results indicate that there is good agreement between the two methods for the open section of the beam, but that the finite element method is not predicting the large differential in torsional stiffness between the open and closed hull sections. This result is consistent with other finite element studies of structures with discontinuous torsional stiffness in the St-Venant sense. Evidently, the good agreement in Pedersen's results of Figure 14 was obtained using full transverse membranes at every nodal cross-section to minimize the in-plane distortion.<sup>(7)</sup> That level of stiffening was not practicable in the present model, but it is anticipated that the addition of full transverse membranes in the model would yield better comparative results.

The necessity of providing transverse stiffness underscores the importance of the thin-walled beam theory assumption of no in-plane distortion, as well as the large contribution such stiffness makes to the overall torsional rigidity. In fact, the introduction of such stiffness in the finite element models is not completely legitimate in the sense that the response of two different physical models is being compared. It must be concluded that the thin-walled theory will provide somewhat optimistic results for beams which do not possess a reasonable degree of in-plane stability; however, in the application of the beam theory method to a typical ship hull structure, an assumption of small distortion would be more appropriate because of the large in-plane stability provided by the numerous transverse bulkheads and deep web frames.

Figure 18 indicates that, despite the poor agreement in twist angle, the axial stress results compare quite favourably. The discontinuity attracts a somewhat higher stress concentration than the beam theory method predicts. The axial stress contours for the top surface of the test beam are shown in Figure 19. The stress concentration at the discontinuity is very apparent.

Anticipating at least representative predictions of displacement and stress, the flexural-torsional beam method has been applied to a study of the static response of the hull of

a frigate under torsional loading. A detailed data base available for this ship allowed the formation of a very representative beam model for use in the torsional analysis. Although a number of reasonably large discontinuities exist in the hull chosen for analysis, only the two most serious were used in the current study. Since a hydrodynamically derived load distribution was not available for this analysis, a distribution given in Lloyds Register<sup>(22)</sup> has been used as a representative load case. This moment distribution is given, in kn-m, as;

$$m(x) = 9.81e^{-0.00295L} \frac{LB^3C_T}{10000} (1.75 + 1.5 \frac{\epsilon}{D})(1 - \cos \alpha) \quad (193)$$

where  $\epsilon$  represents the offset of the shear center below the structure baseline (keel),  $D$  is the ship depth,  $L$  the total ship length between perpendiculars, and  $C_T$  is a coefficient related to the water plane area coefficient,  $C_W$ , as;

$$C_T = 13.2 - 43.4C_W + 78.9C_W^2 \quad (194)$$

with n

$$C_W = 0.165 + 0.95C_B \quad C_B \geq 0.6 \quad (195)$$

The traditional harmonic variation is given by the cosine term, where,

$$\alpha = 2\pi \frac{x}{L} \quad (196)$$

The two major components of this formula attempt to account for the variation of vertical hydrostatic pressure in quartering seas as well as the twisting moment created by the horizontal force resultant about an offset shear center. Substituting the appropriate parameters for the frigate hull, we obtain the moment distribution presented in Figure 20.

The twist angle predictions for the frigate hull for runs with no discontinuities and two discontinuities are presented in Figure 21. Evidently, the inclusion of discontinuities has little effect in this case. (This was not the case in the Pedersen beam, Figure 14.) Figures 22 and 23 present the axial warping stress distributions resulting from this load for sections aft and forward of the first discontinuity respectively, where the warping induced stresses are expected to be highest. These distributions indicate that despite the large geometric discontinuity, the axial stress levels are quite low. Figures 24 and 25 illustrate the differences in the shear stress distributions predicted by a traditional analysis and that provided by the warping beam theory for the section in the vicinity of the deck cut-out. Again, the maximum stress levels are quite low in either case.

## 6 Conclusion

This report has presented a unified development of the thin-walled beam theory and several refinements of that theory adopted for use in ship structural strength analysis. The

various assumptions underlying each formulation have been set out, and their consequences discussed. The introduction of the general warping function, and the formulation of several iterative methods to attempt to account for the secondary shear deformation have been presented. It has been shown that the former refinement leads to unsatisfactory local equilibrium conditions, whereas the latter is computationally more intensive and, in the case of at least one method, can give non-convergent solutions. On that basis, it is not evident that the use of the iterative methods is necessarily worthwhile. As well, certain results as evidenced in Figure 17 appear to indicate that the assumption of no geometric deformation is a far more inaccurate assumption than that of negligible secondary shear strain.

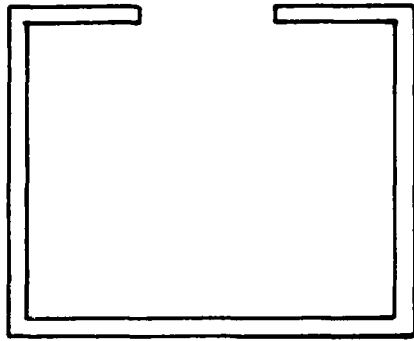
Despite the problems associated with the refinements of the theory, the sectorial based warping formulation provides, in general, a better model of the behaviour of prismatic thin-walled sections because of the account of longitudinal deformation. The non-localized axial and secondary shear stresses associated with warping restraint can add significantly to the overall stress distribution, particularly in open sections with low St-Venant stiffness. Since ship hulls can have significant variations of torsional rigidity due to geometric discontinuities, it is worthwhile to apply these methods to better understand the state of stress in the hull, and the application of these prismatic beam theories to the analysis non-prismatic ship hulls has been discussed. In several of these methods, the ship is idealized as a series of prismatic segments, and improved compatibility of warping displacements between the segments can be obtained through the use of coupling coefficients. For typical warship hulls, these coefficients appear to have little effect on the static displacement or stress predictions.

For singly symmetric structures such as ship hulls, horizontal flexure and torsion are coupled, and a derivation of the static equilibrium equations from an energy variational has been presented. This approach assumes the structure to be a slowly varying beam, and relies on unverified simplifying assumptions to form a tractable solution method. A system of four coupled differential equations requiring numerical solution methods is derived. A computer based analysis system based on this theory has been implemented at DREA for ship hull torsional strength evaluation. Using this system, a number of prismatic test structures have been studied, and the results compared to those of finite element solutions. These comparisons indicated that the thin-walled beam theory assumption of complete in-plane stability is an unrealistic one for unstiffened structures, and very optimistic displacement and stress predictions will be provided by that theory for structures without significant in-plane stiffness. This assumption appears to be a major limitation in the potential applications of the beam method. In cases where a large degree of configurational stability is present, the beam method should provide representative behaviour of the structure under torsional loads. This will be the case for a typical warship hull, because of the large number of deep web frames and transverse bulkheads.

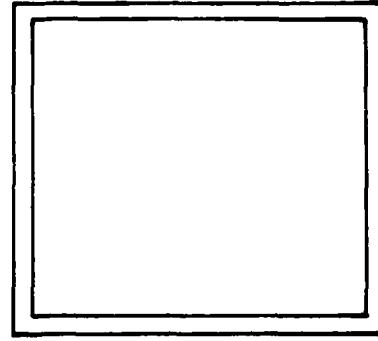
The flexural-torsional beam method has been applied in the analysis of a frigate hull

under a hypothetical torsional load, and the results indicated that quite low stresses are generated in the hull from the prescribed load. Such low stresses are a result of several factors, the most important being the large torsional stiffness inherent in the cellular configuration typical of most warships. It is concluded that normal detailing practices at geometric discontinuities in the hull would be more than adequate to compensate for any stress concentrations caused by axial or shear stresses in torsion.

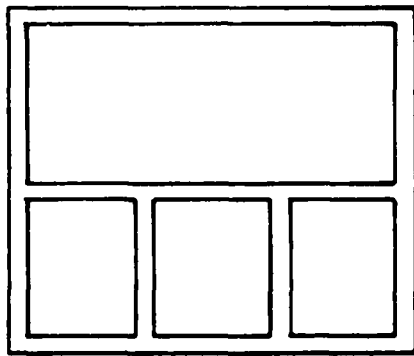
There are several areas described in this report which could benefit from further investigation and development. Specifically, a more general method of coupling the segment warping displacements in non-prismatic beams than the rigid body displacement approach commonly in use could be developed. As well, the importance of the many terms ignored in the strain energy derivation for the slowly varying beam should be investigated. Finally, and perhaps most critically, better descriptions of maximum torsional and flexural loads for ship hulls are required.



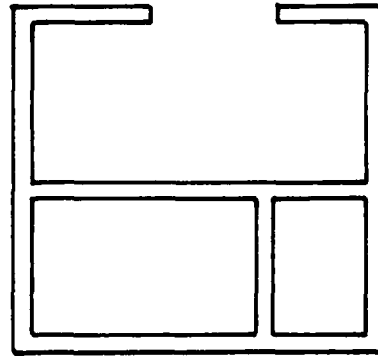
OPEN



CLOSED



MULTI-CELL



MIXED

Figure 1: Open, closed and multi-cell thin-walled beams.

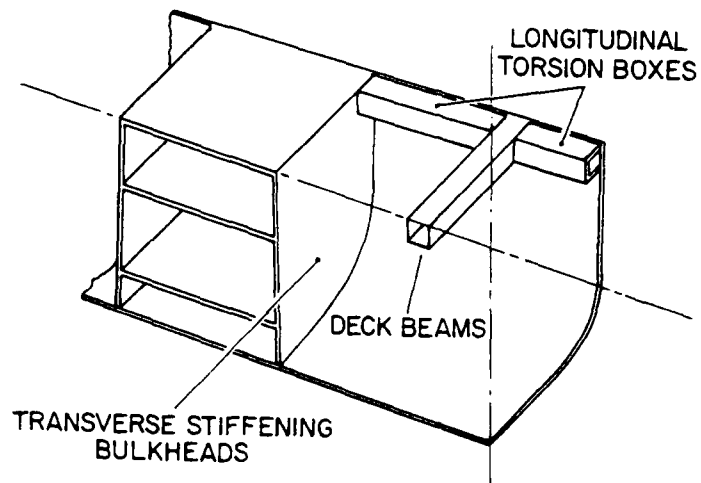


Figure 2: Torsion restraints in a hull form with large discontinuities.

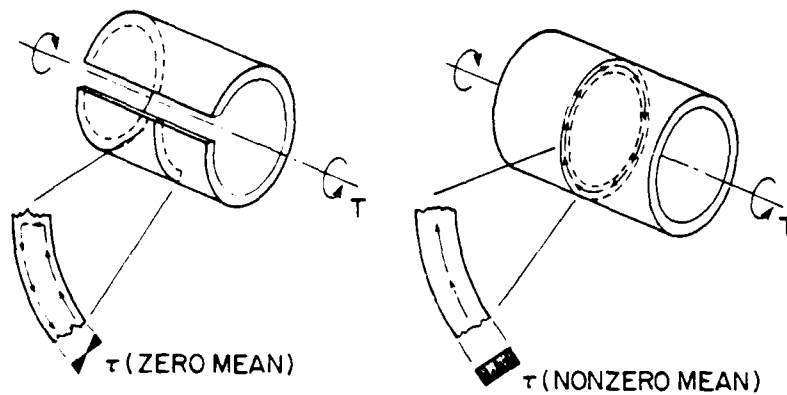


Figure 3: St-Venant shear stresses on open and closed sections.





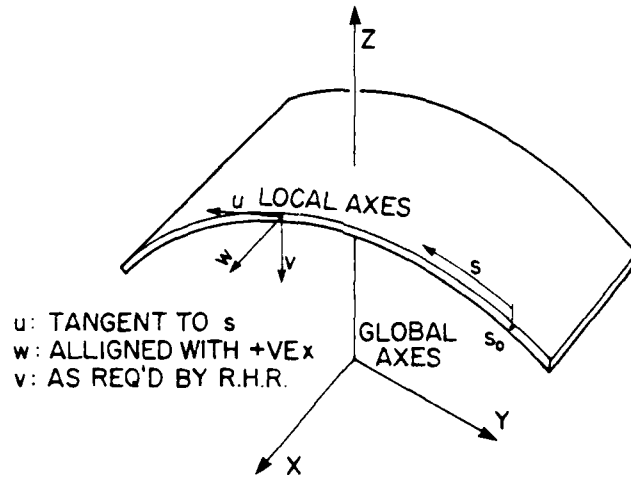


Figure 8: Global and local coordinate systems.

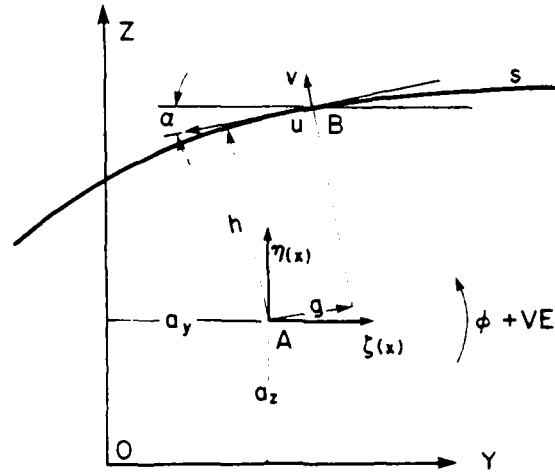


Figure 9: Generalized cross-sectional displacement definitions.

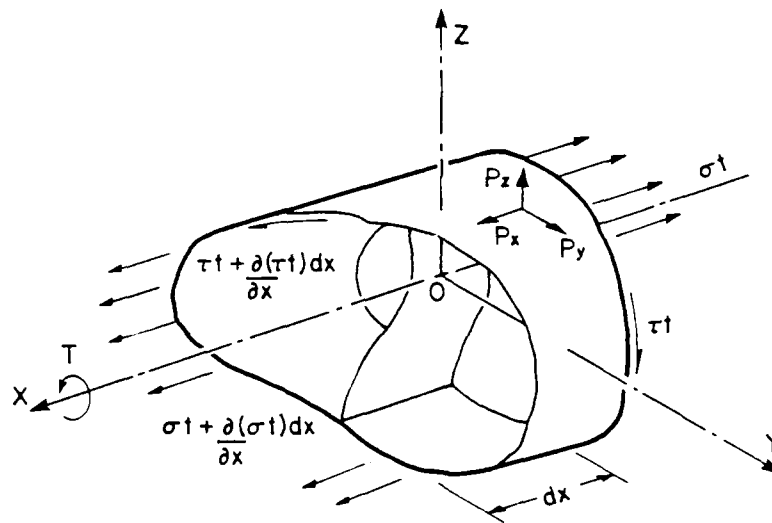


Figure 10: Forces on a wall segment.

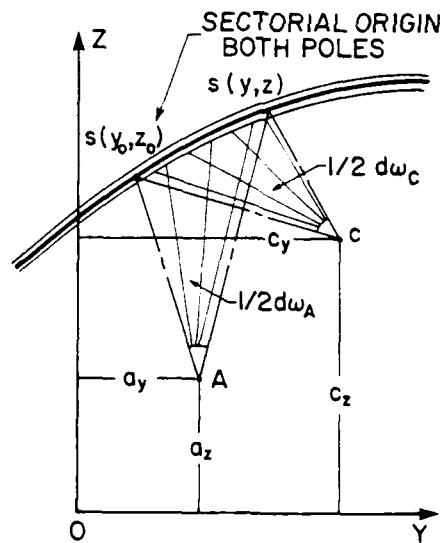


Figure 11: Transfer of sectorial coordinate pole and origin.

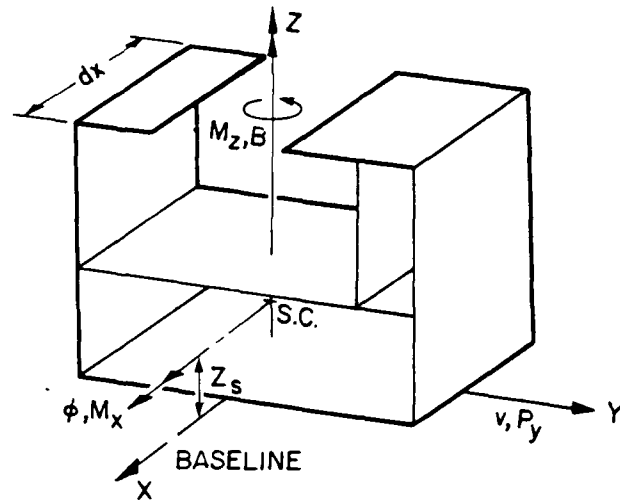


Figure 12: Coordinate system for the flexural-torsional model.

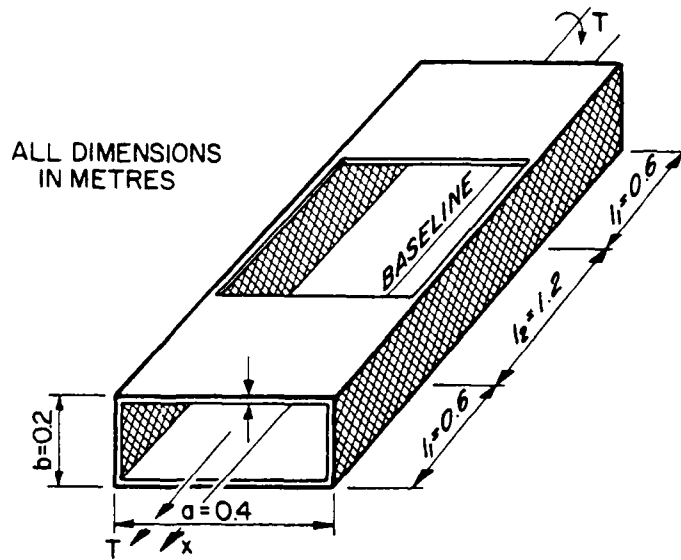


Figure 13: Test 1: Simple box beam with discontinuity.

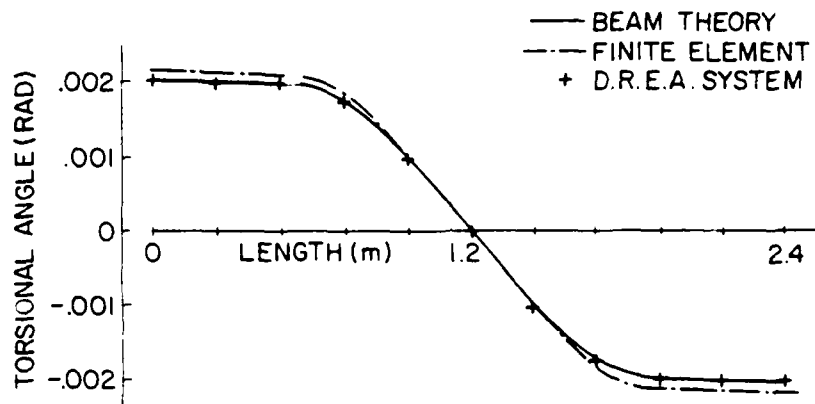


Figure 14: Twist angle predictions for test 1 under a torsional load (Pedersen).

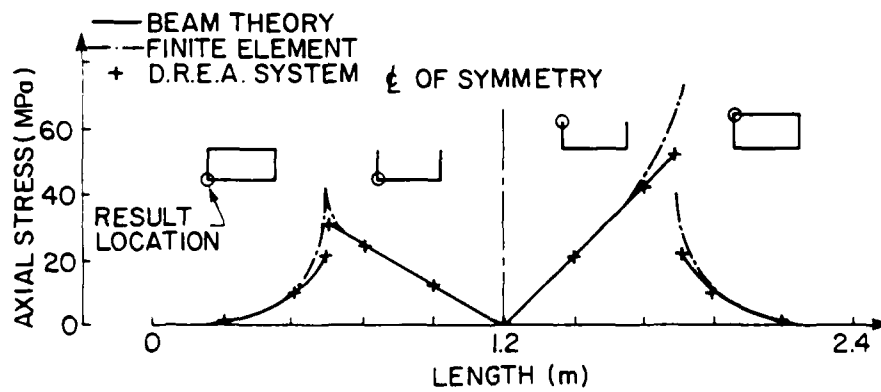


Figure 15: Axial stress predictions for test 1 under a torsional load (Pedersen).

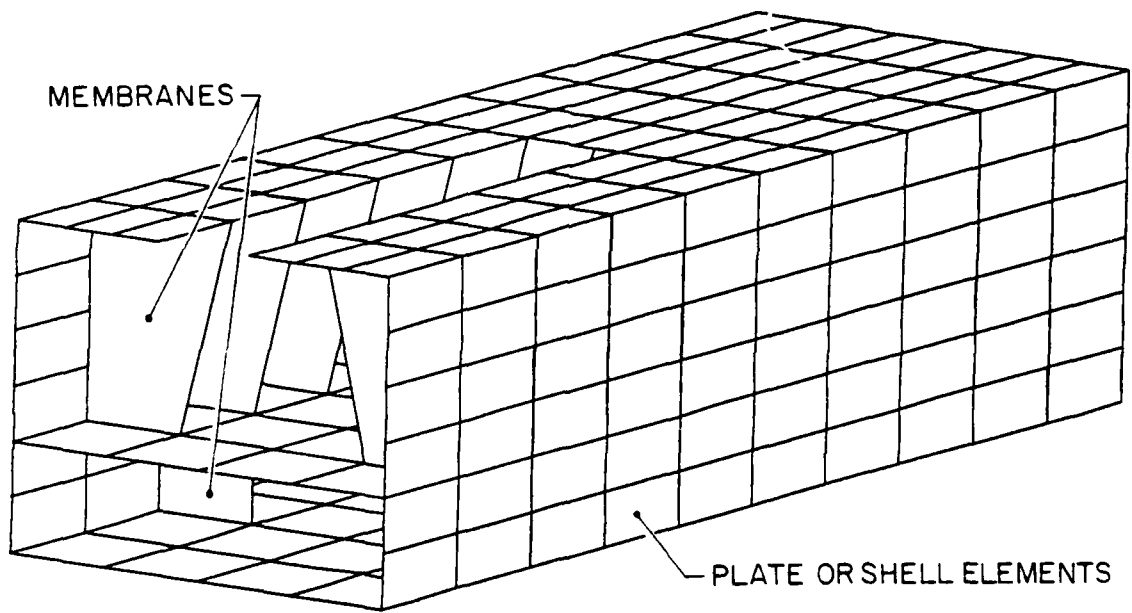


Figure 16: Test 2: Finite element model for comparison solution.

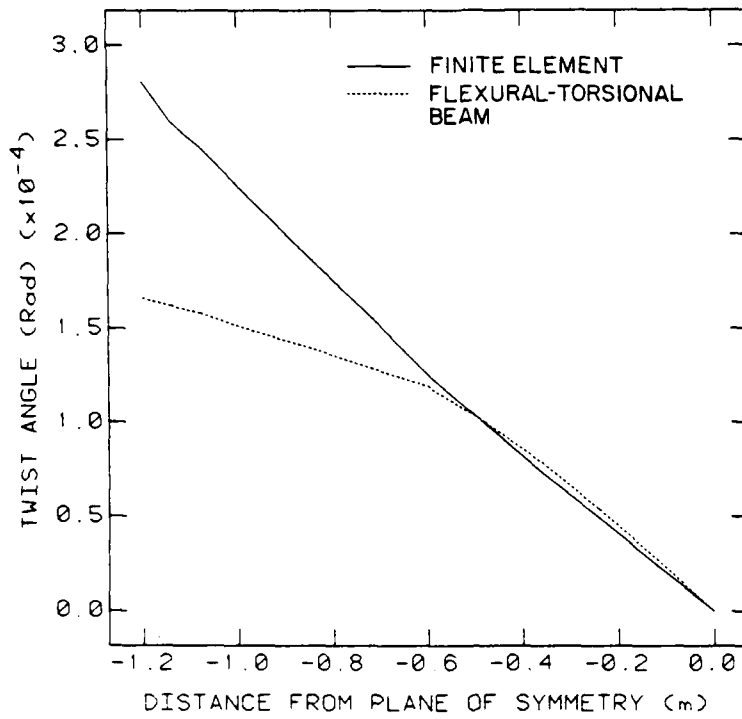


Figure 17: Twist angle predictions for test 2.

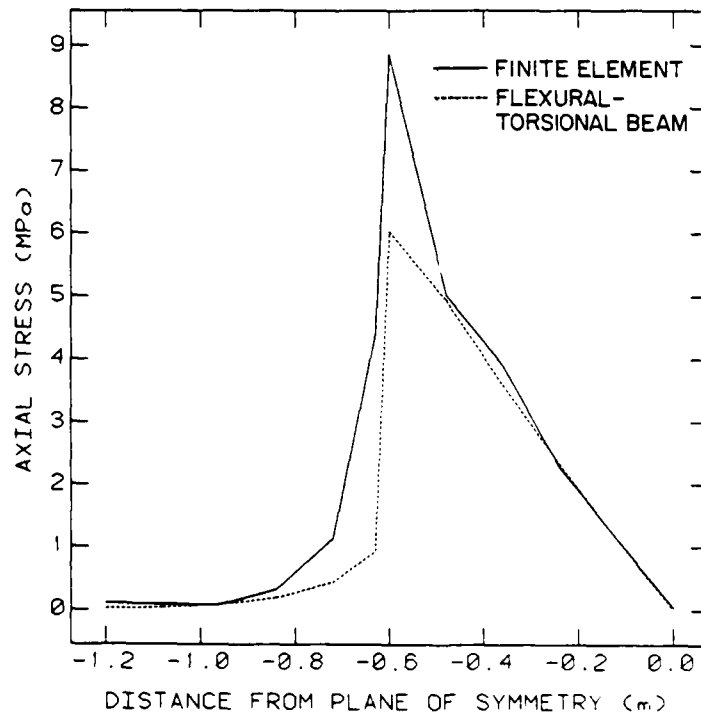


Figure 18: Axial stress predictions for test 2.

AXIAL STRESS  
CONTOURS  
(STATIC ANALYSIS)

STRESS LEVELS

CODE	STRESS MPa
1	-8.000E+00
2	-7.000E+00
3	-6.000E+00
4	-5.000E+00
5	-4.000E+00
6	-3.000E+00
7	-2.000E+00
8	-1.000E+00
9	0.
10	1.000E+00
11	2.000E+00
12	3.000E+00
13	4.000E+00
14	5.000E+00
15	6.000E+00
16	7.000E+00
17	8.000E+00

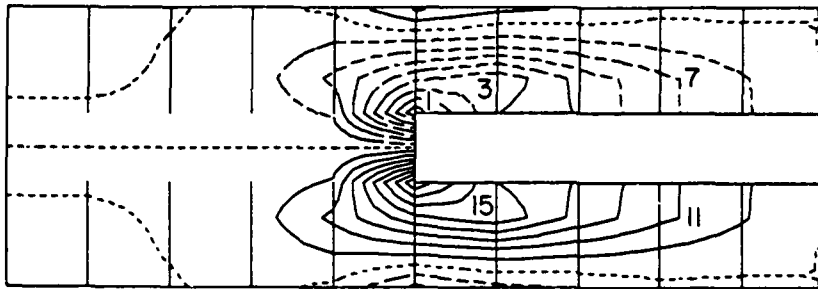


Figure 19: Axial stress contours of top surface showing stress concentration at the discontinuity.

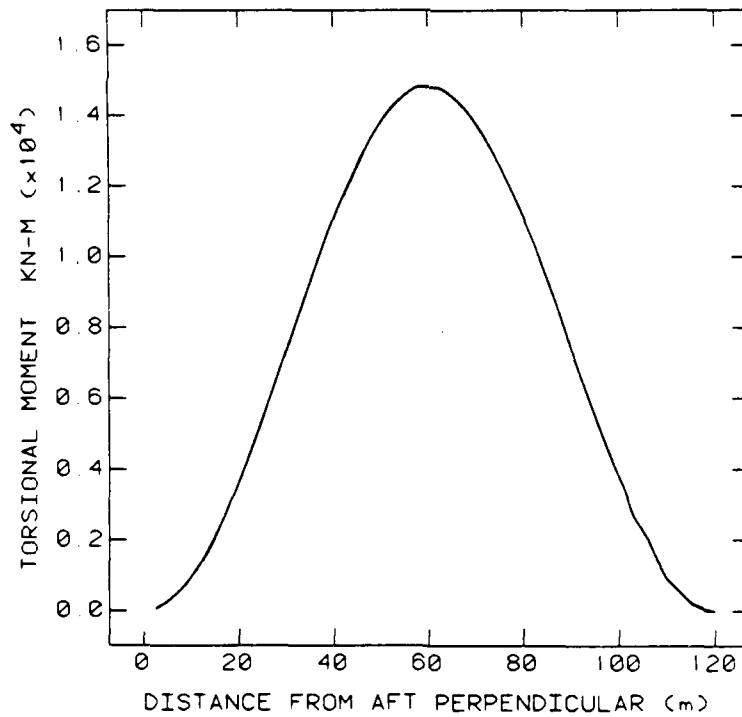


Figure 20: Moment distribution applied to the frigate hull.

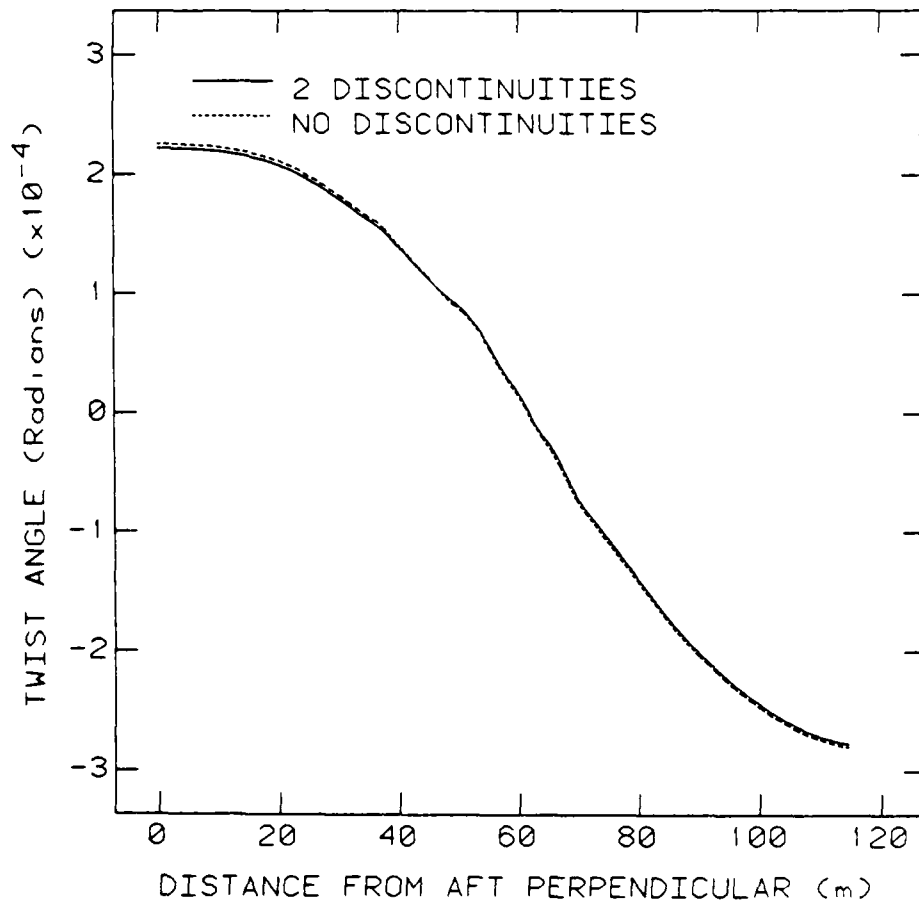


Figure 21: Twist angle prediction for the frigate hull.

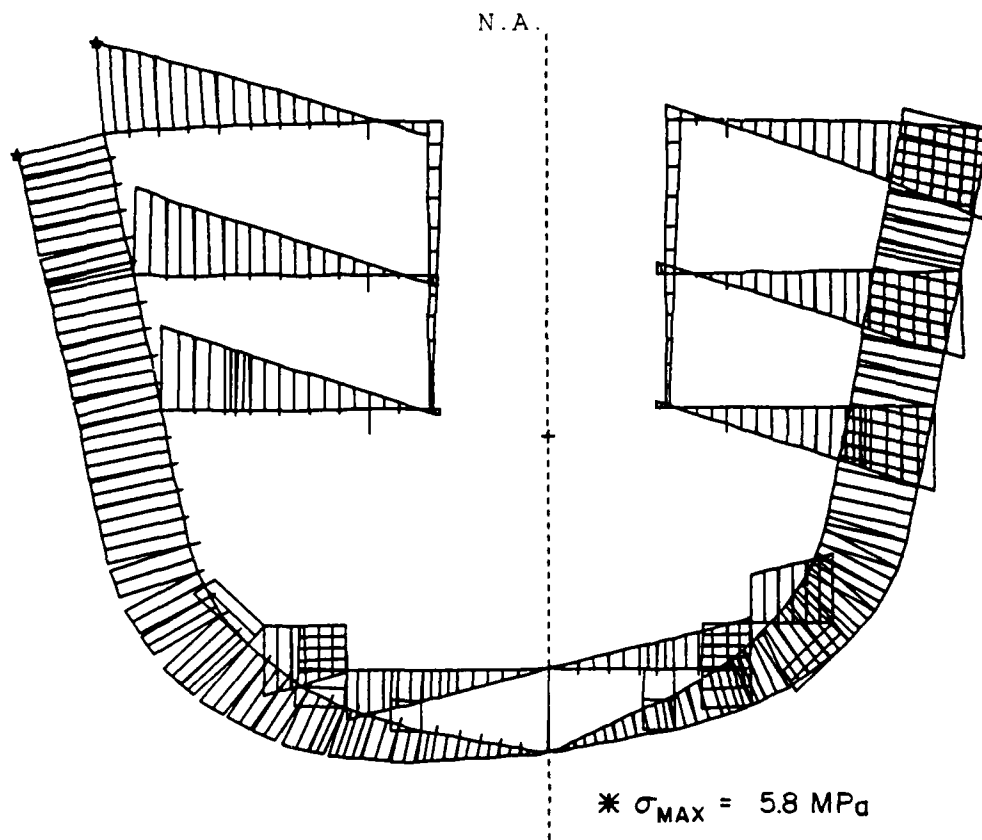


Figure 22: Axial stress immediately aft of the major discontinuity in the frigate hull

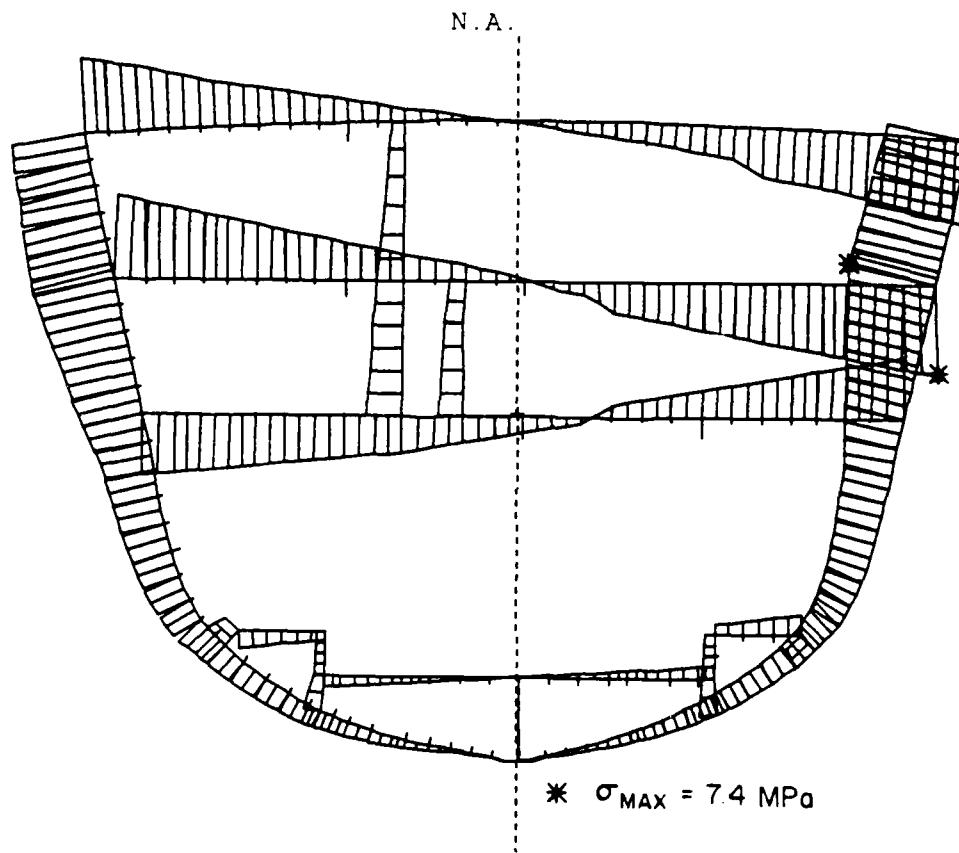


Figure 23: Axial stress immediately forward of the major discontinuity in the frigate hull.

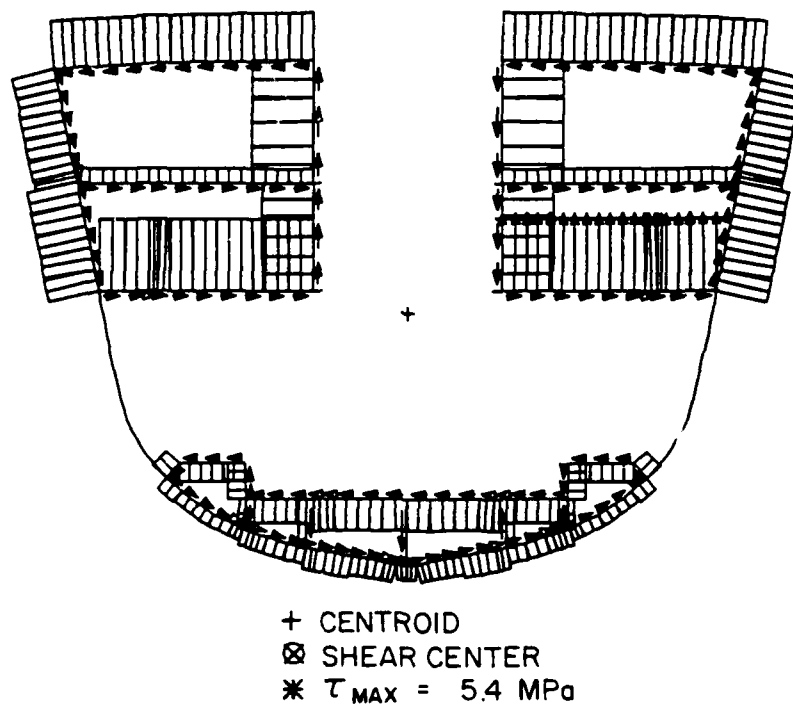


Figure 24: Shear stress distribution from a traditional analysis for a cross-section of the frigate hull.

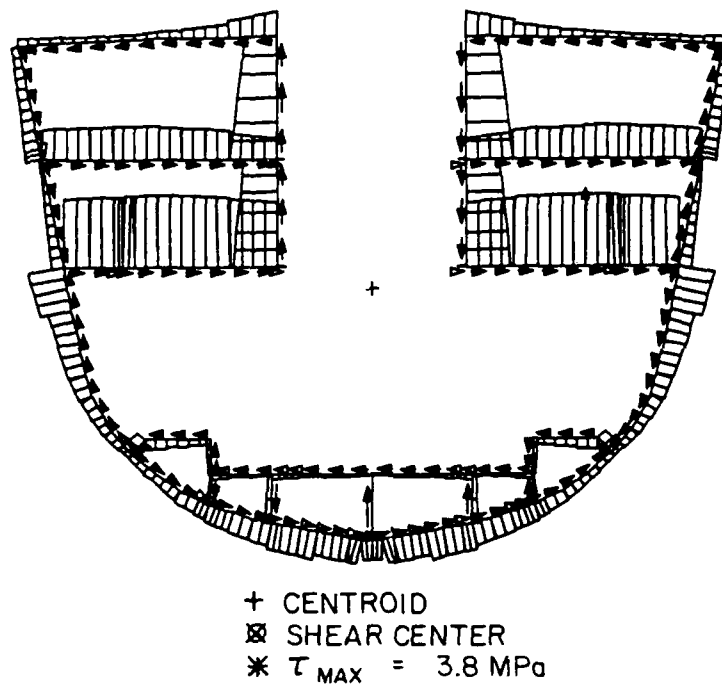


Figure 25: Shear stress distribution from the warping based methods for a cross-section of the frigate hull.

## Appendix A - Notes on the Differential Equation

The classical differential equation of warping torsion in a thin-walled beam is given as,

$$EI_{\omega\omega}\phi'''' - GI_t\phi'' = m(x) \quad (197)$$

where  $m$  represents the external couple per unit length along the beam. Defining the non-dimensional parameter,  $k$ , as,

$$k = \sqrt{\frac{GI_t}{EI_{\omega\omega}}}l \quad (198)$$

equation (197) can be written,

$$\phi'''' - \frac{k^2}{l^2}\phi'' = \frac{m(x)}{EI_{\omega\omega}} \quad (199)$$

The fundamental solution of this linear, inhomogeneous differential equation is obtained by assuming a solution form  $\phi = e^{rx}$  and solving the characteristic equation for the roots  $r$ . This leads to a general solution of the form,

$$\phi(x) = C_1 + C_2(x) + C_3 \sinh \frac{kx}{l} + C_4 \cosh \frac{kx}{l} + P(x) \quad (200)$$

The coefficients of the solution can be determined from the boundary conditions of the problem once a particular solution has been established for the given load case. Some common forms include,

concentrated load:

$$m(x) = 0 \quad (201)$$

$$P(x) = 0 \quad (202)$$

uniformly distributed load:

$$m(x) = p_0 \quad (203)$$

$$P(x) = -p_0 \frac{k^2 x^2}{2l^2 EI_{\omega\omega}} \quad (204)$$

sinusoidal distribution:

$$m(x) = A \sin \frac{\pi x}{l} \quad (205)$$

$$P(x) = \frac{Al^4 \sin \frac{\pi x}{l}}{EI_{\omega\omega} \pi^2 (\pi^2 + k^2)} \quad (206)$$

Four boundary conditions are required, two per beam end, to establish the complete solution. These conditions can be in the form of kinematic or statical constraints. Some

common conditions include,

clamped end:

$$\phi = \phi' = 0 \quad (207)$$

free to warp but not rotate:

$$\phi = M_\omega = 0 \quad (208)$$

free end:

$$M_\omega = T = 0 \quad (209)$$

Other boundary conditions and combinations are possible, such as linear relations between statical and kinematic variables to reflect elastic support conditions. Reference 12 provides a very complete presentation of the various load and boundary conditions.

It is instructive to consider the influence of the parameter  $k$ , which characterizes the elastic properties of the thin-walled beam. As an example, consider the axial stress distribution for a clamped-free beam under a concentrated torsional end moment. In that case, the complete solution of the differential equation (199) is given as,

$$\phi = \frac{T}{GI_t} \left[ x + \frac{l}{k} \tanh k \left( \cosh \frac{kx}{l} - 1 \right) - \frac{l}{k} \sinh \frac{kx}{l} \right] \quad (210)$$

and hence, from the development of Section 3, the axial warping stress distribution is given by,

$$\sigma(x, s) = \frac{Tl}{I_{\omega\omega}k} \left( \sinh \frac{kx}{l} - \tanh k \cosh \frac{kx}{l} \right) \omega(s) \quad (211)$$

Plotting the non-dimensionalized axial stress then gives a description of the attenuation of that stress with length. This has been done in Figure A1 for various values of the parameter  $k$ . It can be seen that the stress decays in at least a linear fashion for this particular case. The higher the value of  $k$ , the more localized is the area influenced by the bimoment stress field. In the limiting case of  $k = \infty$ , the stress is completely concentrated at the restraint. Although the decay characteristics of the axial stress are a function of the load and boundary conditions, this trend is universal.

The value of  $k$  depends mainly on three characteristics of the beam: thickness, length, and geometric configuration. It can readily be shown that  $k$  decreases with decreasing thickness by consideration of the St-Venant and warping stiffness dependence on that variable. Also evident is the importance of the overall beam length; again, in the limiting case of an infinitely long beam, the warping stresses become completely localized. Not as evident is the configurational dependence, and it is difficult to estimate a priori the ratio of the St-Venant and warping torsional rigidities for complex geometries.

Despite the fact that typical warship hulls are quite cellular and hence have large St-Venant torsional rigidities, the  $k$  values in the regions of large deck openings can be quite

low. Assuming that the ends of the cut-out zone are essentially fixed against warping because of their larger St-Venant stiffness, and using the length of the cut-out as a length parameter,  $k$  values of 0.12 and 0.11 are obtained for the two major discontinuities in the CPF hull. Warping restraints in these areas will therefore cause axial and secondary stresses of a non-localized nature.

According to the principle of St-Venant, stresses developed in a section through the application of a balanced external load are localized, and diminish rapidly away from the point of load application. Such a principle should apply to the self-balancing force system of the bimoment distribution. However, because of the relatively slow decay of these axial stress systems, particularly in thin-walled beams of open section, and the nature of the distortion caused by these stresses, the application of the St-Venant principle to such structures is not valid.

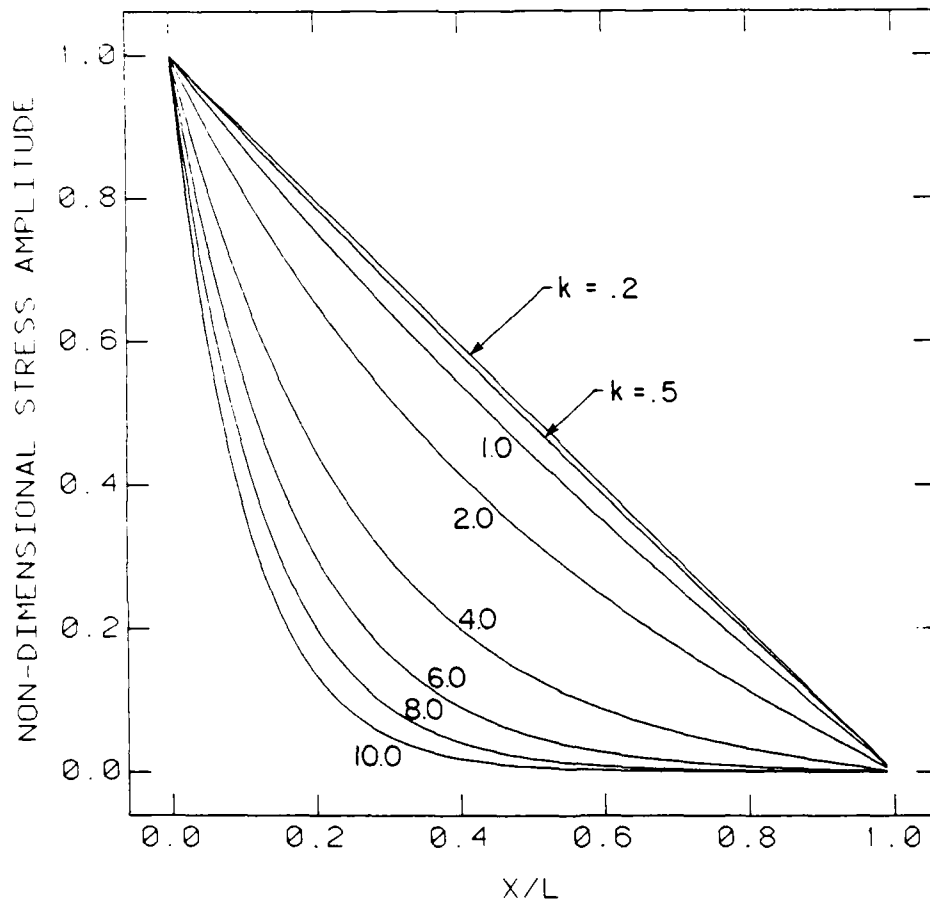


Figure A1: Axial stress distribution for various  $k$  values in a clamped-free beam under a concentrated end moment.

## References

1. Kollbrunner, C.F., Hajdin, N., 'Warping Torsion of Thin-walled Beams of Closed Cross-section', Cement and Concrete Association Translation, Maisel, B.I., 1984.
2. Westin, H., 'Torsion of Non-Prismatic Beam Girders with Special Applications to Open Ships', TRITA-SKP-1055, Div. of Naval Architecture, Royal Institute of Technology, Stockholm, 1980.
3. Pittaluga, A., 'Recent Developments in the Theory of Thin-Walled Beams', Computers and Structures, Vol. 9, 1978, pp. 69-79.
4. Pedersen, P.T. 'A Beam Model for the Torsional-Bending Response of Ship Hulls', Transactions, RINA, 1983.
5. 'Vibration and Strength Analysis of Ship Hulls and Appendages by Finite Element Methods (HVASt)', User's manual, DREA contract OAD 3217048, Martec Ltd., Nova Scotia, 1983.
6. Vernon, T.A., 'SCRAP, A Computer Program for Elastic Strength Analysis and Equivalent Beam Modelling of Ship Hulls', DREA Technical Memorandum 86/214, 1986.
7. Pedersen, P.T., private communication
8. Principles of Naval Architecture, Society of Naval Architects and Marine Engineers, New York, N.Y., 1977.
9. Popov, E.P., Introduction to Mechanics of Solids, Prentice-Hall Inc., Englewood Cliffs, N.J., 1968.
10. Peery, D.J., Aircraft Structures, McGraw-Hill, N.Y., 1950.
11. Marshall, R.W., 'Shear Flow Distribution in Multi-Cell Girders', Computers and Structures, Vol. 4, 1974, pp. 307-325.
12. Vlasov, V.Z., Thin-Walled Elastic Beams, Israel Program for Scientific Translations, U.S. Department of Commerce, 1961.
13. Haslum, K., Tonnesen, A. 'Torsion of Thin-Walled Nonprismatic Beams', Meddelelse SK/M 22, Div. of Ship Structures, Technical University of Norway, Trondheim, 1971.

14. Ulfvarson, A., 'Studies on the Structural Behaviour of Open Ships Under Torsion', Report E-46, Div. of Naval Architecture, Royal Institute of Technology, Stockholm, 1975.
15. Kawai, T., 'The Application of Finite Element Methods to Ship Structures', Computers and Structures, Vol. 3, 1973, pp. 1175-1194.
16. Gunnlauggsson, G.A., Pedersen, P.T., 'A Finite Element Formulation for Beams with Thin Walled Cross-sections', Computers and Structures, Vol. 15, No. 6 1982, pp. 691-699.
17. 'Conversion of TORSION.BAS Program to Fortran 77', DREA contract report, OSC-97707, Martec Ltd., Nova Scotia, 1985.
18. Lewis, F.M., 'The Inertia of Water Surrounding a Vibrating Ship', Trans. SNAME, Vol. 37, 1929.
19. 'Vibration and Strength Analysis Program (VAST), Version 4', DREA contract reports, Martec Ltd., Nova Scotia, 1986.
20. Vernon, T.A., 'SCRAP - Operational notes', DREA internal communication, 1985
21. Vernon, T.A., 'Comparisons Between Finite Element and Beam Theory Analyses of Thin-walled Beams in Torsion', DREA informal communication, 1986.
22. Lloyds Register of Shipping, Rules and Regulations of the Classification of Ships, Part 4, London, 1978.

## Bibliography

1. Kollbrunner, C.F., Basler, K., Torsion in Structures, Springer-Verlag, Berlin, 1969.
2. Pedersen, P.T. 'Torsional Response of Containerships', J. of Ship Research, Vol. 29, No. 3, 1985, pp. 194-205.
3. Hughes, O.F., Ship Structural Design, John Wiley, N.Y., 1983.
4. Vajravelu, P., 'Torsional Strength and Rigidity of 'Open' Ships', Shipping World and Ship Builder, August, 1970.
5. Kawai, T., 'Studies on the Ultimate Strength Analysis of a Ship Structure by means of a New Discrete Thin-Walled Beam Element', J. of Society of Naval Architecture of Japan, Vol. 150, 1982, pp. 381-388.
6. Haslum, K., Tonnessen, A., 'An Analysis of Torsion in Ship Hulls', European Shipbuilding, No. 5/6, 1972, pp. 67-90.
7. Haslum, K., Pedersen, B., 'Torsional Response of a Ship in the Seaway with Particular Reference to an LNG Tanker', Norwegian Maritime Res., Vol. 1, No. 3, 1973.

UNLIMITED DISTRIBUTION

Unclassified  
Security Classification

DOCUMENT CONTROL DATA - R & D		
(Security classification of title, body of abstract and indexing annotation must be entered when the overall document is classified)		
1 ORIGINATING ACTIVITY Defence Research Establishment Atlantic	2a. DOCUMENT SECURITY CLASSIFICATION Unclassified	
	2b. GROUP	
3 DOCUMENT TITLE Thin-Walled Beam Theories and Their Applications in the Torsional Strength Analysis of Ship Hulls		
4 DESCRIPTIVE NOTES (Type of report and inclusive dates) Technical Memorandum		
5 AUTHOR(S) (Last name, first name, middle initial) Vernon, Thomas, A., and Nadeau, Y.		
6 DOCUMENT DATE JANUARY 1987	7a. TOTAL NO. OF PAGES 72	7b. NO. OF REFS 22
8a. PROJECT OR GRANT NO.	9a. ORIGINATOR'S DOCUMENT NUMBER(S) DREA TECHNICAL MEMORANDUM 87/202	
8b. CONTRACT NO.	9b. OTHER DOCUMENT NO.(S) (Any other numbers that may be assigned this document)	
10 DISTRIBUTION STATEMENT UNLIMITED DISTRIBUTION		
11 SUPPLEMENTARY NOTES	12. SPONSORING ACTIVITY	
13 ABSTRACT <p>Unified developments of the St-Venant and warping-based thin-walled beam theories and their application in the torsional analysis of ship structures are presented. Open cell, closed cell and multi-cell configurations are treated. The warping-based torsional theory, which accounts for out-of-plane displacements and displacement restraints, provides axial stress distributions resulting from bimoments and in general offers improved predictions of shear stress distribution in thin-walled beams over the St-Venant theory; however, the use of that theory necessitates a more detailed cross-sectional property evaluation. The generalization of the warping function to a displacement field independent of the twist is discussed, as are several iterative methods of including warping shear deformations. The application of the prismatic warping theory to the analysis of non-prismatic beams is discussed, and the flexural-torsional beam method proposed by Pedersen is developed. This method, in conjunction with a computer program to calculate the required cross-sectional properties, has been integrated into a general torsional stress analysis capability within Defence Research Establishment Atlantic (DREA). The DREA system, which can account for geometric discontinuities in a structure, has been developed as an alternative to finite element methods, and is evaluated here via comparison with detailed finite element analyses for several prismatic beams with discontinuities. The flexural-torsional model appears to give representative behaviour only for structures which possess considerable transverse rigidity. Finally, the beam theory is applied to the stress analysis of the hull of a frigate. The shear and axial stresses predicted for the applied torsional load are quite low, despite the existence of significant geometric discontinuities in the hull.</p>		

KEY WORDS

Thin-walled beams  
 Torsion  
 Torsional analysis  
 Ship structures  
 Ship strength  
 Ship hull

INSTRUCTIONS

1. **ORIGINATING ACTIVITY** Enter the name and address of the organization issuing the document.
- 2a. **DOCUMENT SECURITY CLASSIFICATION** Enter the overall security classification of the document including special warning terms whenever applicable.
- 2b. **GROUP** Enter security reclassification group number. The three groups are defined in Appendix 'M' of the DRB Security Regulations.
3. **DOCUMENT TITLE:** Enter the complete document title in all capital letters. Titles in all cases should be unclassified. If a sufficiently descriptive title cannot be selected without classification, show title classification with the usual one-capital-letter abbreviation in parentheses immediately following the title.
4. **DESCRIPTIVE NOTES.** Enter the category of document, e.g. technical report, technical note or technical letter. If appropriate, enter the type of document, e.g. interim, progress, summary, annual or final. Give the inclusive dates when a specific reporting period is covered.
5. **AUTHOR(S):** Enter the name(s) of author(s) as shown on or in the document. Enter last name, first name, middle initial. If military, show rank. The name of the principal author is an absolute minimum requirement.
6. **DOCUMENT DATE:** Enter the date (month, year) of Establishment approval for publication of the document.
- 7a. **TOTAL NUMBER OF PAGES:** The total page count should follow normal pagination procedures, i.e., enter the number of pages containing information.
- 7b. **NUMBER OF REFERENCES.** Enter the total number of references cited in the document.
- 8a. **PROJECT OR GRANT NUMBER:** If appropriate, enter the applicable research and development project or grant number under which the document was written.
- 8b. **CONTRACT NUMBER** If appropriate, enter the applicable number under which the document was written.
- 9a. **ORIGINATOR'S DOCUMENT NUMBER(S):** Enter the official document number by which the document will be identified and controlled by the originating activity. This number must be unique to this document.
- 9b. **OTHER DOCUMENT NUMBER(S):** If the document has been assigned any other document numbers (either by the originator or by the sponsor), also enter this number(s).
10. **DISTRIBUTION STATEMENT:** Enter any limitations on further dissemination of the document, other than those imposed by security classification, using standard statements such as:
  - (1) "Qualified requesters may obtain copies of this document from their defence documentation center."
  - (2) "Announcement and dissemination of this document is not authorized without prior approval from originating activity."
11. **SUPPLEMENTARY NOTES** Use for additional explanatory notes.
12. **SPONSORING ACTIVITY:** Enter the name of the departmental project office or laboratory sponsoring the research and development. Include address.
13. **ABSTRACT:** Enter an abstract giving a brief and factual summary of the document, even though it may also appear elsewhere in the body of the document itself. It is highly desirable that the abstract of classified documents be unclassified. Each paragraph of the abstract shall end with an indication of the security classification of the information in the paragraph (unless the document itself is unclassified) represented as (TS), (S), (C), (R), or (U).  
  
The length of the abstract should be limited to 20 single-spaced standard typewritten lines, 7 1/4 inches long.
14. **KEY WORDS:** Key words are technically meaningful terms or short phrases that characterize a document and could be helpful in cataloging the document. Key words should be selected so that no security classification is required. Identifiers, such as equipment model designation, trade name, military project code name, geographic location, may be used as key words but will be followed by an indication of technical context.

END

4-87

DTIC